ENZYMATIC DEGRADATION OF SELF-ASSEMBLED PEPTIDE NANOFIBER GELS

A THESIS SUBMITTED TO

THE GRADUATE SCHOOL OF ENGINEERING AND SCIENCE

OF BILKENT UNIVERSITY

IN PARTIAL FULFILLMENT OF THE REQUIREMENTS FOR

THE DEGREE OF

MASTER OF SCIENCE

IN

MATERIAL SCIENCE AND NANOTECHNOLOGY

By

Aygül Zengin

February 2016

ENZYMATIC DEGRADATION OF SELF-ASSEMBLED PEPTIDE NANOFIBER GELS
By Aygül Zengin
February 2016

We certify that we have read this thesis and that in our opinion it is fully adequate, in scope and in quality, as a thesis for the degree of Master of Science.

Mustafa özgür Güler(Advisor)

Ayşe Begüm Tekinay

Erhan Bat

Approved for the Graduate School of Engineering and Science:

Levent Onural
Director of the Graduate School

ABSTRACT

ENZYMATIC DEGRADATION OF SELF-ASSEMBLED PEPTIDE NANOFIBER GELS

Aygül Zengin
M.Sc. in Material Science And Nanotechnology
Advisor: Mustafa özgür Güler
February 2016

The self-assembled peptide nanofiber gels have received enormous attention because of their inherent biocompatible, biodegradable and functional properties. They provide a smart platform for a range of applications such as tissue engineering, drug delivery and wound healing.

These gels are formed through noncovalent interactions such as hydrogen bonding, hydrophobic interactions and electrostatic interactions among the peptide amphiphile molecules at physiological conditions. In order to understand the stability of these gels in the presence of proteases in natural conditions, we studied degradation behavior of the gels with proteinase K, which is a non-specific protease cleaving the peptide bonds. Degradation process was studied by measuring weight measurement and TEM imaging. In addition, sustained release of Rhodamine B from these gels was also studied in the presence of proteases. The results clearly demonstrated that presence of D- amino acids in the peptide nanofiber network significantly improves their stability against enzymatic degradation and change the release profile of the encapsulated molecules in the gels. These findings are interesting for biomedical applications of these materials due to their tunable degradation and controlled release behavior.

Keywords: Peptide amphiphile, self-assembly, supramolecular gel, nanofiber, D-amino acids, controlled release, enzymatic degradation.

ÖZET

KENDİLİĞİNDEN BİR ARAYA GELEN PEPTİT NANOFİBERLERDEN OLUŞAN JELLERİN ENZİMATİK DEGREDASYONU

Aygül Zengin
Malzeme Bilmi ve Nanoteknoloji, Yüksek Lisans
Tez Danışmanı: Mustafa özgür Güler
şubat 2016

Kendiliğinden bir araya gelen peptit nanofiber jeller, doalar gerei biyouyumlu, biyobozunur ve biyofonksiyonel özelliklerinden dolayı son derece ilgi çekmektedirler. Bu yapılar, doku mühendisliği, ilaç salımı ve yara iyileşmesi gibi çeşitli uygulamalar için akıllı bir platform oluştururlar.

Bu jeller, fizyolojik koşullarda peptit amfifil molekülleri arasındaki hidrojen bağı, hidrofobik ve elektrostatik etkileşimler gibi kovalent olmayan etkileşimler aracılığıyla oluşturulmuştur. Bu jellerin, proteaz içeren doğal koşullardaki stabilitesini anlamak için jellerin degredasyon davranışı,spesifik olmayan bir şekilde peptit bağlarını kıran bir proteaz olan proteinaz K ile çalışılmıştır. Degredasyon prosesi, ağırlıktaki azalmayı ölçerek ve TEM görüntülemesi kullanarak yapılmıştır. Ek olarak, proteinaz K varlığında, rodamin B'nin bu jellerinden sürekli salımı çalışılmıştır. Sonuçlar, D- peptit moleküllerin jel ve nanofiber ağında bulunmasıyla, bu yapıların enzimatik degredasyona karşı kararlılıklarının arttığını ve jel içinde hapsedilen moleküllerin salım profillerinin değiştiğini açıkça göstermiştir. Elde edilen bu bulgular, ayarlanabilir degredasyon ve kontrollü salım davranışları açısından bu malzemelerin biyomedikal uygulamaları için önemlidir.

Anahtar sözcükler: Peptit amfifil, kendiliğinden bir araya gelme, supramoleküler jel, nanofiber, D-amino asitler, kontrollü salım, enzimatik degredasyon.

Acknowledgement

I would like to express my appreciations to my advisor Prof. Mustafa özgür Güler for his guidance and support during the course of this thesis. I would like to express my special thanks to Prof. Ayşe Begüm Tekinay for sharing her knowledge.

I would like to thank to my colleagues and my senior peers Dr. Ruslan Garifullin, Dr. Özlem Erol, Göksu Çinar, Gülcihan Gülseren, Gülistan Tansık, Melis Şardan and Mohammad Aref Khalily for helpful discussions.

I would like to express most sincere thanks to friends; Meryem Hatip, Türkan Bayrak, Seda Kizir. Their support always motivated me. In addition, special thanks to my officemates, Hepi Hari Susapto, Zeynep Aytaç, Aslı çelebioğlu, Yelda Ertaş, Fatma Kayacı, Zehra İrem Gürbüz. They helped me to work in such a warm environment.

I would like to special thank to my best buddies, Ali Torun, Benan İnan, Hatice Köse, Belma Nural and Sinem Yakarsönmez. We shared unforgettable memories together and I always felt their support including my high school and undergraduate years. I would like to thank my flat mates, Gökçe Aydoğan and Pelin Gülizar Ersan. I would like to thank Ulaş Kudu for his support and help.

I would like to thank to Mr. Mustafa Güler and Ms.Zeynep Erdoğan for technical assistance and helpful discussion.

I would like to thank TÜBİTAK (The Scientific and Technological Research Council of Turkey) for grant numbers 114Z728, 214Z214 and BİDED-2210C fellowship.

Finally, I would like to express my most sincere gratitude to my family. I am eternally grateful for supporting and allowing me to pursue my ambitions throughout my life. Thank you for letting me be the person I am today.

To the first kernel of corn with the courage to pop

Contents

List of Figures

List of Tables

Chapter 1

Introduction

1.1 Self-Assembled Peptide Nanostructures

Molecular self-assembly is a powerful bottom-up approach for creating highly ordered structures. Weak non-covalent bonds including hydrogen bonds, ionic bonds, hydrophobic interactions, and van der Waals interactions have significant roles in mediating the structural conformation of molecules and controlling their interaction with other molecules. Nature has already utilized this path to generate hierarchically functional materials from a wide range of building blocks such as proteins, lipids, or DNA. The greatest advantage of this approach is creating nanostructures at multiple length scales and controlling their final architecture precisely by altering their molecular chemistry through modifying environmental conditions such as temperature, pH, and ionic strength. [13, 14]

Peptides are versatile building blocks for fabricating a wide range of self-assembling nanostructures for various applications due to their intrinsic biocompatible, biodegradable and biofunctional properties. The variety in the nanostructures which are formed by self-assembled peptides comes from the capability of the peptides of making use of different molecular interactions such as hydrophobic interactions, hydrogen bonding, electrostatic interactions and aromatic interactions. [15]

Secondary structures of peptides have major role in their organization into highly ordered, supramolecular architectures. The main types of secondary structures are the α-helix, β-sheet, β-hairpins and coiled coils. (Figure 1.1)α-Helix is the most common protein secondary structure where amino acids are prone to form hydrogen bonds between the carbonyl groups and amide groups for promoting peptide backbone stabilization. Compared to β-sheet conformations, α-helix based assemblies have a tendency to be reversible. However, they can form more stable conformations by coming together with other α-helix structures. Until today, numerous α-helical based nanostructures were developed for various purposes. [1, 12, 16]

Coiled-coils are the most extensively studied α-helical structural motifs. They

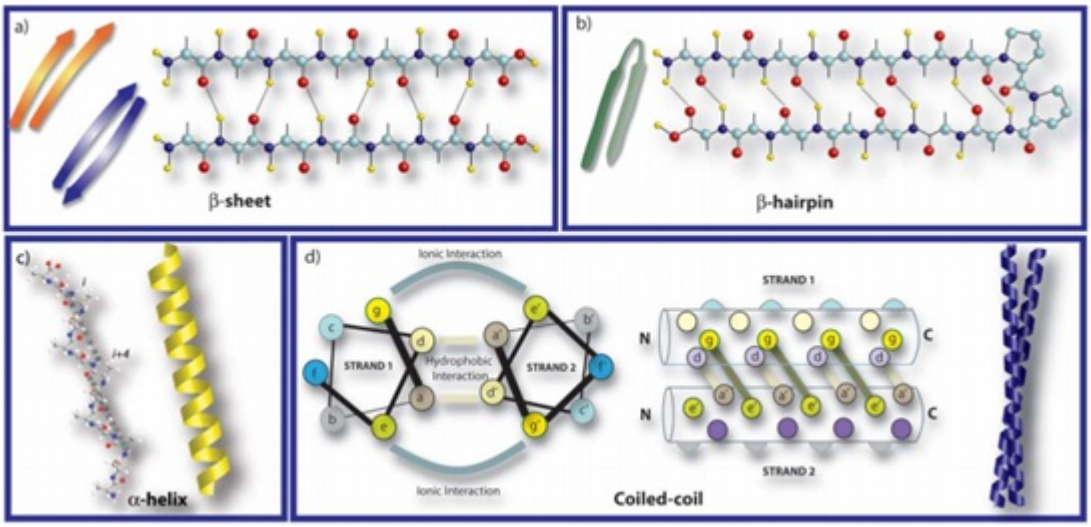

Figure 1.1: Illustration of main types of peptide secondary structures. (a) β-sheet, (b) β- hairpin, (c) α-helix and (d) coiled-coil (Reproduced from Ref [1] with permission of the PCCP Owner Societies 2013)

contain 2-5 helices which are wrapped around each other. Basically, coiled-coil nanostructure formation is based on repeated heptad units, -abcdefg-, in the peptide sequence. The amino acids in positions at a and d promote hydrophobic interactions and e and g provide electrostatic interactions in order to obtain the secondary structure formation. Such peptide sequences can assemble into a variety of nanostructures such as nanofibrils or nanoparticles with the contribution of hydrophobic and electrostatic interactions. [1, 12, 16]

The β-sheet is the second widely studied secondary structure form which arises from laterally connected β-stands through hydrogen bonds. Hydrogen bonding between the carbonyl and amine groups and hydrophobicity stabilizes this structure. They can be either parallel, which means two- β-sheet components aligned in the same direction, or antiparallel aligned in the opposite direction. Peptides have a tendency to form β-sheets and self-assemble into various supramolecular architectures such as nanofibers, nanovesicles, nanotubes. [1, 12, 16]

The β-hairpin is another secondary structure motif which arises as the short loop segments between antiparallel hydrogen bonded β-stands. They are typically found in globular proteins. β-hairpin loop conformation changes according to its

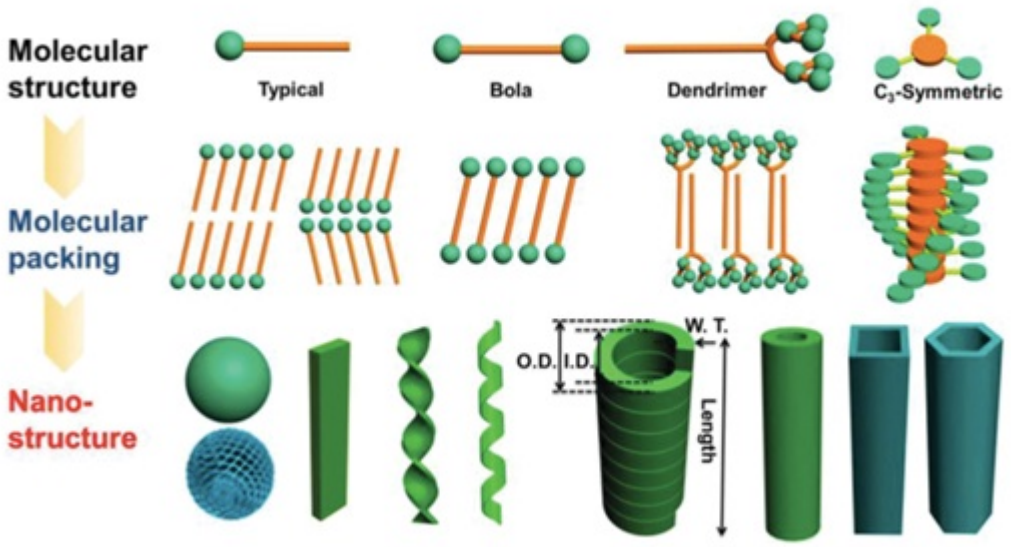

Figure 1.2: Various self-assembled peptide nanostructures (Reproduced from Ref [2] with permission of John Wiley and Sons 2015)

length and sequence. [1, 12, 16]

With the help of synthetic methods, it is possible to create a wide range of peptide based supramolecular nanostructures with different morphologies including fibers, tubes, vesicles, tapes and ribbons. (Figure 1.2) These specific nanostructures can arise from several factors such as chemical structures and order of building blocks, molecular packaging properties, and environmental conditions such as pH, temperature, ionic strength and aging time. [2]

1.1.1 Solid Phase Peptide Synthesis

Solid phase peptide synthesis (SPPS) is a commonly used approach to readily synthesize peptides by coupling the carboxyl group of one amino acid to the amino group of another with high purity and yield. Pioneering work of Merrifield related to solid-phase peptide synthesis caused radical change within the peptide synthesis society in 1963. [17]

SPPS enables to generate proteins and peptides artificially in the laboratory

conditions. Particularly, it is useful for synthesis and design of unnatural amino acids containing peptides or natural complex peptides which are expressed in bacteria. However, chain length and sequence of amino acids (particularly amyloid peptide synthesis) influence the yield of this method. [18]

The main logic behind the SPPS is a stepwise elongation an amino acid sequence on a solid polymer bead through sequential steps of coupling and deprotection of protected amino acids. At the end of this process, elongated peptide is removed from these polymer beads which are called resin. These small beads provide a suitable environment which holds the peptide chain robustly until cleaved by a reagent, for instance trifluoroacetic acid. Widely used solid polymer supports for peptide synthesis based on Fmoc chemistry are 4-hydroxymethylphenyloxymethyl polystyrene resin developed by Wang, 4-hydroxymethylphenoxyacetyl-poly (dimethylactylamide) resin developed by Atherton, and 2-chlorotritylchloride (CTC) resin developed by K. Barlos. Figure 1.3 gives an overview of solid phase peptide synthesis principles. [19–21]

There are two major strategies of SPPS: Fmoc/tBu and Boc/Bzl. [22–24] Recently, Fmoc- chemistry has become more favorable than Boc-chemistry because of its safe and mild environmental conditions. 9-Fluorenylmethoxycarbonyl (Fmoc) represents the Fmoc protecting group. In order to get rid of the Fmoc group from a growing peptide sequence, basic conditions which are generally 20% piperidine in DMF are employed. Incubation with trifluoroacetic acid (TFA) promotes removing side-chain protecting groups and peptide chain from the polymer bead. [25, 26]

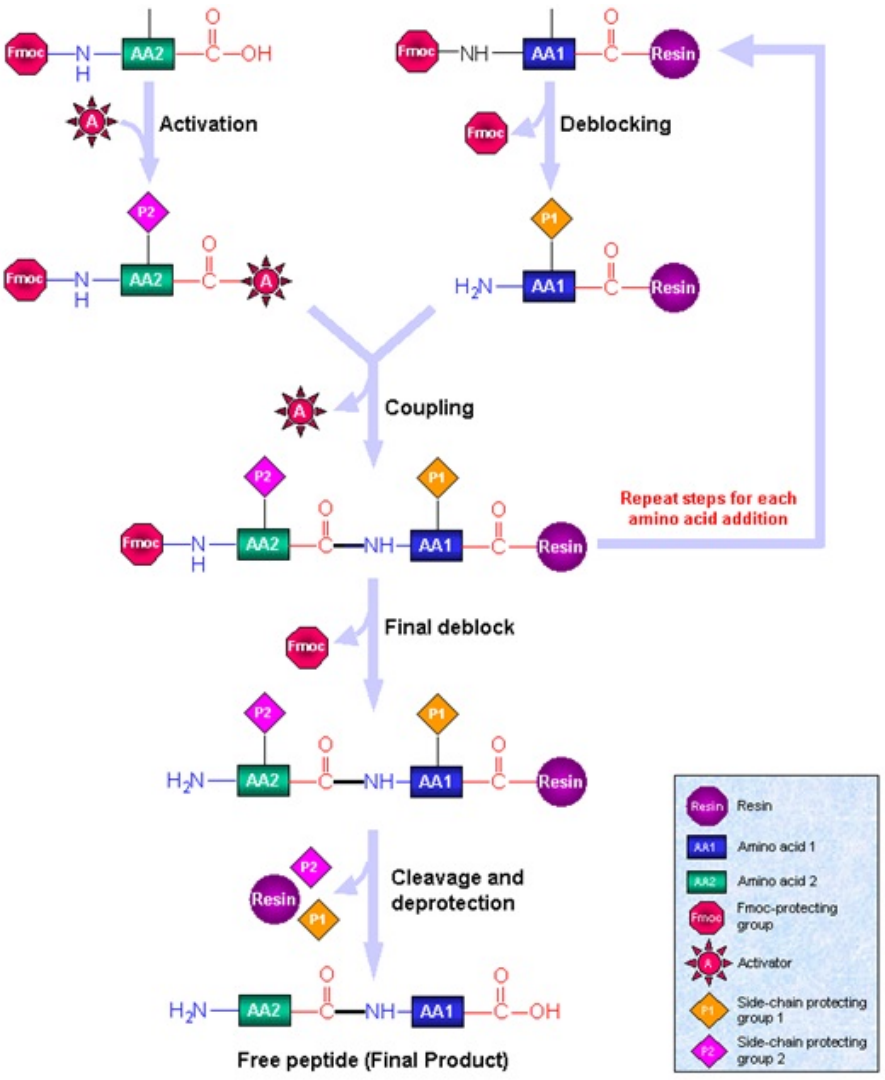

Figure 1.3: Basic steps of solid phase peptide synthesis (Reproduced from ref [3]).

1.1.2 Characterization Techniques for Self-Assembled Peptide Molecules

Compositional analysis of synthesized peptide molecules can be done by liquid chromatography and mass spectrometry (LC-MS). MS is a very rapid and sensitive technique for analysis of peptide/proteins. Matrix assisted laser desorption and ionization (MALDI) and electrospray ionization (ESI) are the two generally used ionization methods for MS analysis. These techniques can be merged with various mass analyzers (quadrupole, TOF). [27]

Structural analysis of self-assembled peptide molecules can be done by employing circular dichroism (CD) and Fourier transform infrared (FTIR) spectroscopy. CD is used to determine the secondary structure of self-assembled peptides. α-helical, β-sheet, β-turn and random-coil conformations have distinctive dichroic signatures which are easily detected. (Figure 1.4)

Notably, CD offers a great opportunity to monitor secondary structure changes in response to various environmental stimuli such as pH, temperature, and ionic strength. [27]

Fourier transform infrared (FT-IR) spectroscopy is another suitable technique to analyze the secondary structure of self-assembled peptides. Similar to CD, α-helical, β-sheet and random-coil structures have specific absorption peaks. Major advantage of this technique over CD is being less sensitive to light scattering. This may enable to study higher concentrations of peptides. However, TFA salts of peptides and water limits this method because of their strong absorption in the amide I region. In order to achieve these limitations, excess TFA ions of peptides are usually removed by dissolving peptide in 0.1 M HCl solution. Then, lyophilization is employed to exchange water from the environment. [27]

Bulk mechanical properties of self-assembled peptide gels can be investigated by using oscillatory rheology. Mechanical rigidity of gels is typically evaluated by measuring the storage and loss modulus of gels against time, frequency, or strain. Also, detailed information about the physical properties of gels such as

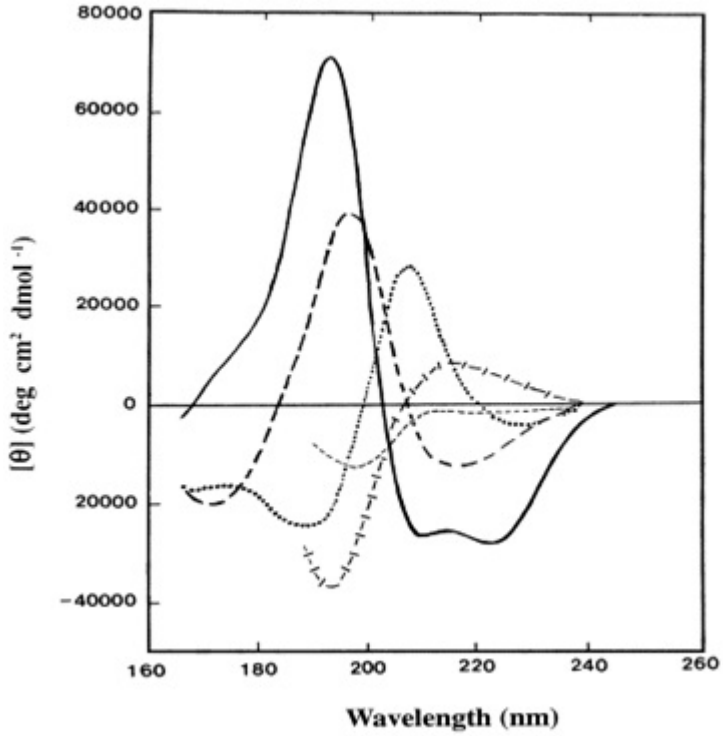

Figure 1.4: Circular dichroism patterns for peptide secondary structures. Solid line, α-helix; long dashed line, anti-parallel β-sheet; dotted line, type I β-turn; cross dashed line, extended α-helix or poly (Pro) II helix; short dashed line, irregular structure. (Reproduced from Ref [4] with permission of Elsevier 2005).

crosslinking, density may be obtained by using rheological measurements. [27]

Morphological characterizations of self-assembled peptide nanostructures can be achieved by using transmission electron microscopy (TEM), atomic force microscopy (AFM) or scanning electron microscopy (SEM). TEM visualizes 2D self-assembled peptide nanostructures. It enables very high resolution by measuring absorption and diffraction of electrons. In general, dilute solutions of self-assembled peptide gels are dropped on copper grids and let dry. Contrast agents such as uranyl acetate are frequently employed to obtain more detailed nanostructures. The major limitation for this technique is hydration. Nanostructures may change after drying and visualized in different from that in the original state. To overcome this potential drawback, cryo-TEM can be performed. [27]

In addition to TEM, atomic force microscopy (AFM) can be an essential instrument in studying self-assembled peptide nanostructures. AFM relies on measurement of force between the cantilever tip and samples surface. It provides information about 3D surface topologies of self-assembled peptide materials. [27]

Scanning electron microscopy is a commonly used electron microscopy technique. It gives valuable information about 2D surface properties of samples. This technique is based on the measurements of scattered electrons. [27]

1.1.3 Applications of Self-Assembled Peptide Nanostructures

Self- assembled peptide nanostructures are attractive candidates for various applications such as regenerative medicine, drug delivery, bioimaging, biomineralization and nanoelectronics. Particularly, biocompatible, biodegradable and biofunctional nature of these materials make them notable for rational design of bioinspired and biomimetic materials. [5, 28] (Figure 1.5)

Self-assembled peptide networks can be used as smart platforms for controlled delivery of drugs and oligonucleotides. In a study, slow release of ODNs was achieved from a nanofibrous platform which was formed by mixing the cationic PAs (C12-VVAGK-Am, Lys-Pa) with Bcl-2 antisense oligonucleotide (ODN) through electrostatic interactions. The results indicated that changing concentrations of PA-ODN mixtures affected the release behavior and PAs also influenced the uptake of ODNs by the cells. [29]In a different study, cell penetrating peptides (CPPs) were employed to encapsulate paclitaxel (PTX), which is a hydrophobic anticancer drug in order to enhance the solubility of the drug and achieve multidrug resistance. As a conclusion, they reported that tat nanofibers may effectively carry encapsulated drug molecules into the cells by use of adsorptive-mediated endocytosis pathway. [30]

Figure 1.5: Self-assembled peptide nanomaterials for a wide range of applications (Reproduced from Ref [5] with permission of John Wiley and Sons 2015).

Self-assembled peptide nanostructures were also used to provide antimicrobial activity. The principle behind this application was that naturally occurring antimicrobial peptides have capability to disrupt the bacterial membrane. One of the first examples towards antibacterial activity belongs to peptide nanotubes. They were used to disrupt the bacterial membrane integrity by forming nanochannels inside and to kill bacteria by osmotic pressure. [31] In addition, it is reported that peptide nanotubes were also employed as a template for fabrication of silver nanowires for possible nanoelectronic applications and electrodes for biosensing. [32, 33]

In the field of bioimaging, magnetic resonance imaging (MRI) is one of the most powerful diagnosis techniques which enables to visualization of 3D structure of the living tissue. The major drawback of this technique is lack of strong contrast agents which promotes prolonged in vivo imaging time. In a pioneering study, Stupp group developed an MR agent-conjugated PA system to enhance the relaxivity. They used a derivative of DOTA which is covalently attached to PAs. It was shown that DOTA conjugated Pas were self-assembled into both spheres and cylindrical nanofibers and the relaxivity of MR agent was increased. [34]

Self-assembled peptide nanostructures can be further used in the regeneration of soft tissues such as blood vessels and skin, and hard tissues such as bone and cartilage. [6, 35]

Table 1.1: Self-assembled peptides as drug delivery vehicles (Reproduced from Ref [12] with permission of American Chemical Society 2016)

Composition/Sequences	Supramolecular Structure	Secondary Structure	Cargo
L-diphenylalanine:NH_2-FF-COOH	Microtubes	–	Rhodamine B
Fmoc-FF-COOH	Hydrogel nanoperticles	–	Doxorucbucin
MAX8:VKVKVKVK-V^DPPTKVEVKVKV-NH_2	Fibrils	β-hairpin	Curcumin
$(AC\text{-}FLIVI)_2KKKKK\text{-}CONH_2$	Nanovesicles	β-sheet	5(6)-carboxyfluorescein
RADA16-I:Ac-$(RADA)_4$-$CONH_2$	Nanofiber hydrogel	β-sheet	Pindolol, Quinine, Timolol maleate
RADA16-I:Ac-$(RADA)_4$-$CONH_2$	Nanofiber hydrogel	–	Human IgG
RADA16-I:Ac-$(RADA)_4$-$CONH_2$	Nanofiber hydrogel	β-sheet	Lysozyme, trypsin inhibitor, IgG, BSA
$SA_{2\text{-}7}$: Ac-AAVVLLLW$(E)_{2\text{-}7}$-COOH	Nanovesicles	PPII	Zinc-phthalocyanine (TT-ZnPcNH_2
RADA16-I:Ac-$(RADA)_4$-$CONH_2$	Nanofiber hydrogel	–	Cytokines: βFGF
Ac-$(RADA)_4$-GGDGEA-$CONH_2$	–	–	BDNF
Ac-$(RADA)_4$-GGPFSSTKT-$CONH_2$	–	–	VEGF
NH_2-PSFCFKFEP-COOH	Nanofibers	β-sheet	Pyrene
MAX8:VKVKVKVK-V^DPPTKVEVKVKV-NH_2	Fibrils	β-hairpin	Lysozyme, α-lactalbumin, myoglobin, lactoferrin
EAK16-II:NH_2-AEAEAKA-KAEAEKAK-COOH	Nanofiber	β-sheet	Ellipticine
EAK16-IV:AEAEAEAEA-KAKAKAK-COOH	Globular nanostructures, short nanofibers	β-turn	
EAK16-II: FEFEFKFKFE-FEFKFK-COOH	Nanofiber	not reported	

1.2 Self-Assembling Peptide Amphiphile Molecules

Peptides are versatile building blocks for fabricating novel materials. Particularly, peptide amphiphiles (PAs) have received broad interest in creating nanoscale, functional biomaterials for various applications. [36, 37]

The PA molecules basically consist of four key elements: (1) a hydrophobic tail, (2) β-sheet forming sequence, (3) charged groups and (4) a bioactive epitope. The first region, hydrophobic tail, is commonly a long alkyl tail such as fatty acids which promotes aggregation through the hydrophobic collapse. It can be adjusted by using different alkyl chain lengths or hydrophobic moieties. This segment allows to present bioactive epitopes on the nanofiber surface. The second region is β-sheet forming sequence which is typically composed of hydrophobic amino acids with high hydrogen-bonding capability in the form of β-sheet. This leads to the formation of one-dimensional (1D) assemblies. The third region derives solubility in water through the charged amino acid residues. To be able to promote nanofiber growth by environmental stimuli such as changing pH or making use of ionic strength, mainly weak acids or bases are used as charged amino acids. The number of these amino acids should be enough to guarantee adequate solubility. Otherwise, electrostatic repulsion between the charged moieties can disrupt the self-assembly mechanism of the PAs. Lastly, the fourth region consists of a bioactive epitope which can be tuned for various purposes such as cell adhesion, cell migration, and differentiation. Since this region presents the opposite end of the hydrophobic tail, bioactive epitopes are easily displayed on the nanofiber surface. [37–40] In neural applications, laminin derived IKVAV sequence is commonly used as an epitope incorporated in to PAs for promoting cell adhesion, cell migration and neurite growth. (Figure 1.6) Another frequently used bioactive epitope is RGDS, which is present in many extracellular matrix (ECM) proteins, and derives cell adhesion. Incorporation of such epitopes in to the PAs provides a biomimetic network resembling ECM. [41–44]

The principle behind the self-assembly of the PA molecules basically relies on

three major forces: Hydrophobic interactions of the alkyl tails, hydrogen bonding between the β-sheet forming sequence and electrostatic interactions among the charged amino acids. Interaction between these forces determines the structural properties such as size, shape and interfacial curvature. [45–47] Stupp group used molecular simulations which are based on only hydrophobic interactions and hydrogen bonding in order to understand PA self-assembly behavior in water. According to this model, only hydrophobic interactions of PA molecules generate micelles of finite size. On the contrary, only hydrogen bonding between the molecules leads to 1D β-sheet. Contribution of both hydrophobic interactions and hydrogen bonding influence the assembly kinetics thanks to changed strength of intermolecular interactions. (Figure 1.7) Characterization of PA assemblies by advance microscopy techniques such as transmission electron microscopy (TEM), scanning electron microscope (SEM), and atomic force microscopy (AFM) demonstrated that they have strong propensity to form cylindrical nanofibers with high-aspect-ratio instead of tapered shape as predicted before. [48, 49]

After the EAK16 peptide motif (AEAEAKAKAEAEAKAK) was found out from a yeast protein Zuotin in 1992, first computational estimations demonstrated that it has α-helix structure since the possible ionic bonds come from lysine and glutamic acid containing side chains. [50]When only the amino acid sequence was changed but not the composition, it was found that this peptide has remarkably steady β-sheet structure. However, later studies have shown that L-EAK16 peptide shows remarkably stable β-sheet structure rather than α-helix. [51,52]In addition, it was reported that this peptide can spontaneously form highly ordered nanofiber structures. Therefore, the first self-assembling peptides were explored. [53]

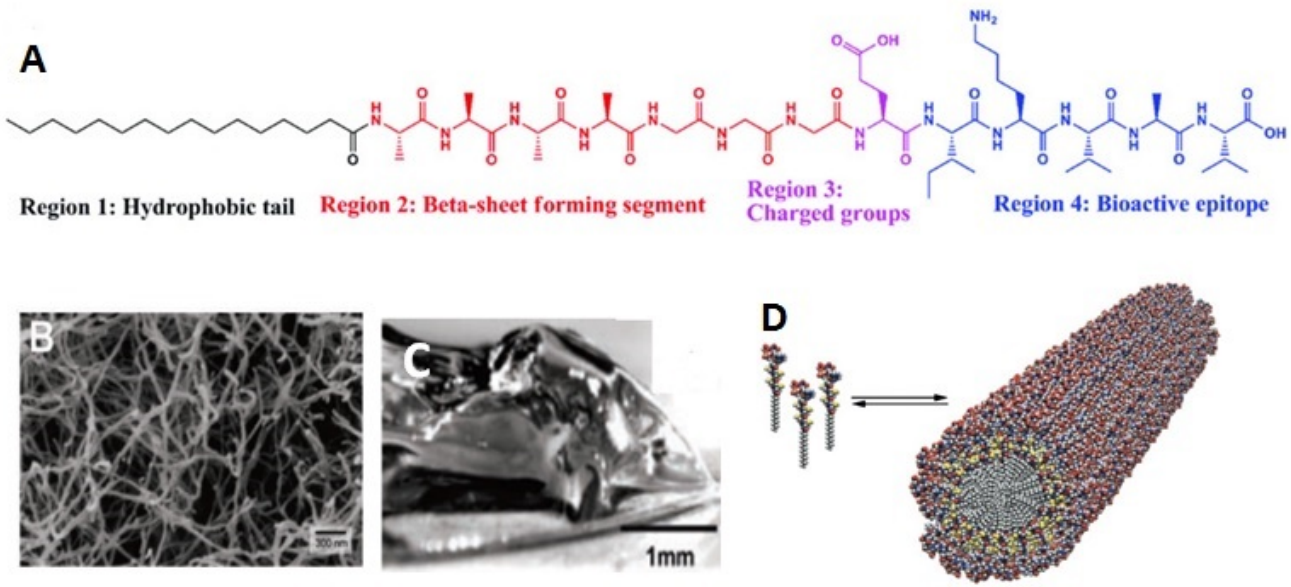

Figure 1.6: Molecular structure of PA nanofibers (a) Chemical structure of IKVAV-PA nanofiber formation, (b) SEM of 3D network IKVAV-PA nanofiber, (c) gel formation by adding cell culture media, and (d) molecular graphics illustration of self-assembly into high-aspect-ratio nanofibers (Reproduced with permission of Ref [6] with permission of The Royal Society of Chemistry).

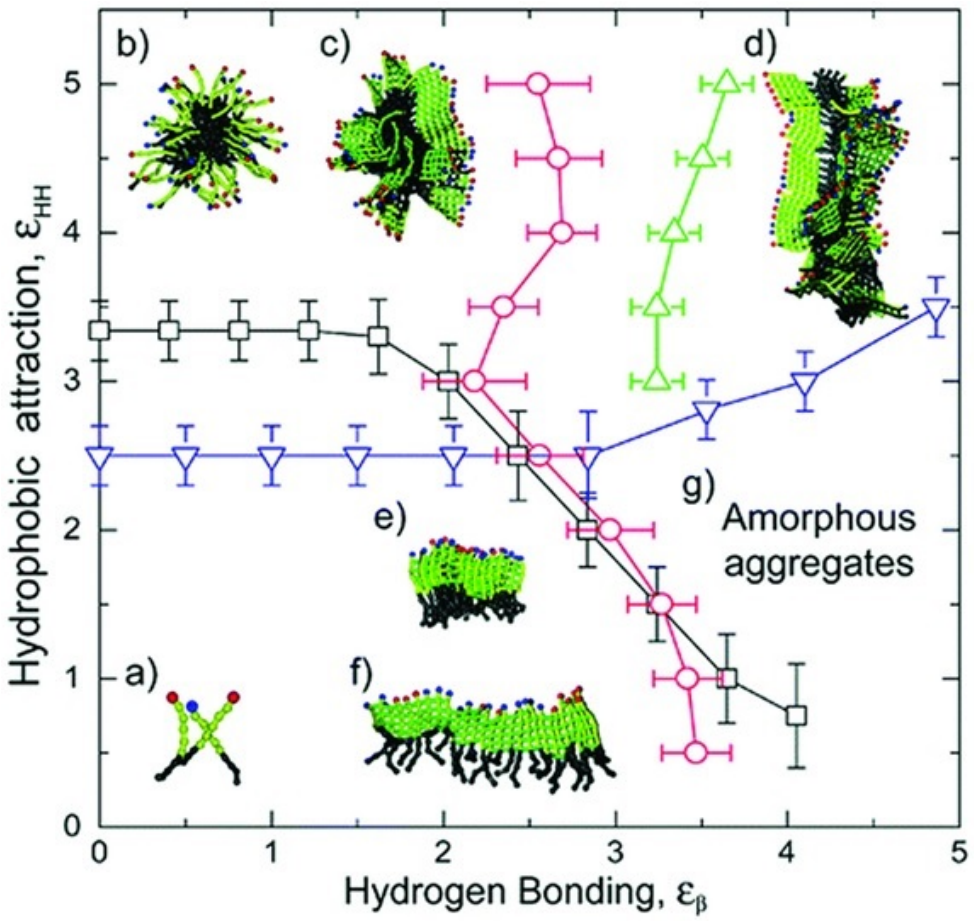

Figure 1.7: Phase diagram of PA self-assembly behavior. (a) free molecules, (b) spherical micelles, (c) micelles with β-sheet, (d) long cylindrical fibers, (e) parallel sheet stacks, (f) single β-sheets and (g) amorphous aggregate phase (reproduced from Ref [7] with permission of American Chemical Society 2008).

After their discovery, various types of self-assembling peptides containing L-amino acids with a variety of amino acid sequences, compositions and lengths have been researched in the past decades. In one work, Luo *et al.* investigated a 16-residue self-assembling peptide d-EAK16 which contains only D-amino acids to explore the change in its structural characteristics at different pH values, temperatures and in the presence of some denaturing chemicals. They reported that changes in the temperature and the pH value trigger the secondary structure transition of d-EAK16 between β-sheet and α-helical conformation. While the secondary structure was β-sheet at 25°C, it turned into α-helix structure when the temperature was raised above 80°C. On the other hand, d-EAK16 peptide demonstrated different secondary structure tendencies in different pH values. Although it displayed α- helix structure at pH 0.76 and pH 12, it formed typical β-sheet structure at neutral pH. Moreover, they reported that there was no significant influence of salt and denaturing agents such as urea, guanidine-HCl, and 0.1% SDS. [8]

Furthermore, Luo *et al.* synthesized hybrid chiral peptides by changing L- and D- amino acids in sequence, EA*K16 and E*AK*16. In this work, the self-assembly behavior was observed to be reduced. Additionally, d-EAK16, EA*K16 and E*AK*16 contributed to wound healing process showing that d-EAK16 was more advantageous in rapid hemostasis than the peptides containing alternating L- and D- amino acids. [54]

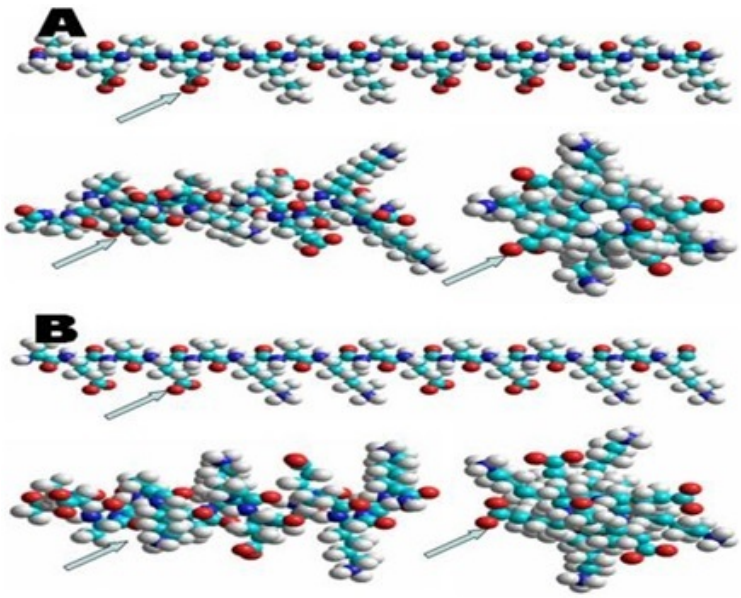

Figure 1.8: Molecular model of d-EAK16 (a) and l-EAK16 (B) (Produced from Ref [8] with permission of Creative Commons Attribution License 2008).

D-form self-assembled peptides are interesting due to their exclusive properties: (i) their stability against enzymatic degradation, (ii) their easily regulated self-assembly process by environmental stimuli, (iii) their ability to rapidly stop bleeding, (iv) and their contribution to sustained cell growth. In an inspiring work, D-form self-assembled peptides were used in 3D cell cultures to examine the relation between the nanofiber network and cell activities. Cell viability on D-form peptides was quite high and there are low-levels of apoptosis. Same behavior was observed in the case of L-peptides. Also, d-EAK nanofibers demonstrated good stability in the presence of different enzymes such as trypsin, pronase, and pepsin as well. On the other hand, rheological studies with L-EAK16 and D-EAK16 in salt solution indicated that d-EAK16 It was more responsive to ions compared to l-EAK16 and this enhances the mechanical properties of d-EAK16. [55] As a conclusion, using chiral D-form self-assembling peptides may trigger creation of new generation biomaterials and promote a variety of applications of D-form self-assembling peptides in the biomedical field.

1.3 Gels for Biomedical Applications

Hydrogels are three-dimensional (3D) polymeric networks that can absorb large amounts of water. They have immense inherent capacity for various tissue engineering and drug delivery applications thanks to their high water content, viscoelastic properties and diffusion properties. Based on the cross linking properties, hydrogels can be divided into two main classes: Chemical (covalent) or physical gels. Traditional synthesis approaches including crosslinking copolymerization, crosslinking of polymeric precursors and polymerpolymer reactions are applied for production of chemical gels. Although various types of hydrogels can be produced by using these methods, they have many disadvantages such as no precise control in the structure, possible toxicity of cross linking procedures and forming of strong irreversible structures as a result of the covalently bound network. In the case of physical hydrogels, molecular network chains are held together by non-covalent interactions such as hydrogen bonding, hydrophobic interactions, and electrostatic interactions. These interactions can be influenced by the environmental changes such as temperature, pH and ionic strength. As a result, non-covalently bound hydrogel matrices may be reversible. [56]

Hydrogels can be composed of a variety of synthetically derived (e.g. polyethylene oxide, polyethylene glycol, polyvinyl alcohol, polyacrylic acid, polypeptides) and naturally derived (e.g. agorase, chitosan, collagen, hyaluronic acid, alginate, fibrin, gelatin) materials. [57] All the materials which are used in hydrogel matrices have their own disadvantages and advantages. Synthetically derived hydrogels provide more controllable and reproducible network architecture and chemical composition. However, they exhibit lower bioactivity. On the other hand, naturally derived hydrogel materials offer great biocompatibility and biodegradability which result in harmless degradation products and inherent biological functionality. But they may not provide adequate mechanical strength and may evoke immune responses. [58] Limited control over the gelation process, mechanical strength and degradation behavior of the natural material based hydrogels has accelerated the development of novel synthetic hydrogels. Recently, peptide based

hydrogel systems which are based on self-assembly of molecules into highly ordered 3D structures in response to changes in ionic strength, temperature, pH or electrostatic interactions has been studied extensively. Owing to their inherent biocompatible and biodegradable characteristics and tunable functionality, they have an important place for various applications such as controlled drug delivery, tissue engineering, wound healing and biosensing. [59, 60](Table 1.2)

Self-assembling hydrogel systems are driven by weak non- covalent interactions such as hydrogen bonding, hydrophobic effect, van der Waals interactions and electrostatic interactions. Self-assembly is a highly specific and smart gelation mechanism as the toxic chemicals are eliminated, and it is possible to trigger cross linking via environmental stimulation and the material properties are more controllable due to reversible nature of the assembly and disassembly processes.45

Self-assembled peptide nanofiber hydrogels form a noteworthy class of peptide based hydrogels. They have many advantages compared to the traditional polymeric hydrogels such as easy gel formation by changing pH, salt concentrations or using oppositely charged nanofibers, tunable mechanical strength, elimination of toxic crosslinking agents and in vivo injectability. There are many studies in the literature to prove that these hydrogels are responsive to external stimulation in promoting triggered assembly, disassembly, or degradation. [61–64]

1.4 Drug Delivery Application of Peptide Gels

Even though there are several approved biopharmaceutical products and ongoing clinical studies, there are still number of restrictions in the administrations of drugs. [65, 66] For instance, the propensity of proteins to be physically or chemically degraded may restrict the therapeutic efficacy, and decrease the drug half-life. [67]To overcome this limitation, hydrogel biomaterials have been utilized as delivery vehicles for protein based drugs. Encapsulation of therapeutics within the gel matrices may enhance the stability towards enzymatic degradation, prolong half-life of drugs and enable controlling over the release rate. [68, 69]

A potential strategy for the design of gel networks is the use of self-assembled molecules which are based on non-covalent interactions such as hydrogen bonding, hydrophobic interactions, electrostatic interactions, and generation of highly ordered nanostructures. Using peptides as molecular building blocks for self-assembly is promising thanks to tunable bulk properties of gels through the programmable amino acid sequence, and their biocompatible and biodegradable characteristics. For instance, with the help of solid phase synthesis method, desired material properties such as mesh size, hydrophilicity/hydrophobicity, and degradation rate may be achieved easily by changing amino acid residues. This enables a smart platform for controlling molecular diffusion by engineered peptide molecules. Additionally, concentration of the peptides which are used for gel formation influences the mesh size of gels and release behavior directly. [70]

Doxorubicin (DOX), camptothecin (CPT) and cisplatin (CDDP) are commonly used drugs for delivery applications. They are toxic for both cancer cells and healthy cells and use passive diffusion to enter the cells. [71]Working principle of these drugs is based on inhibition of DNA synthesis. There are two major ways to decrease the side effects and enhance the therapeutic efficacy by using peptide molecules. One of them is conjugation of peptides with these drugs via amide bonds, ester bonds, hydrozone bonds and enzymatically cleavable bonds. Soudy *et al*. have conjugated to peptides which have high selectivity for breast cancer cells to doxorubicin via ester and amide bonds. Cell uptake studies revealed that the drug-peptide conjugates containing ester bonds were 6-10 times more specific for the cancer cells. Although they showed similar toxicity to free dox against the cancer cells, they were approximately 40 times less toxic to the healthy cells. [72]

Another strategy is encapsulating the drug molecules within the peptide gel networks directly during self-assembly process. For example, Kim *et al*. built a bioresponsive cisplatin (CDDP) delivery platform by using MMP-2 specific self-assembling peptide amphiphile nanofiber gels in order to form a system of CDDP-PA gels, PA molecules and the drug. In order to form the system, the reagents were held at 37°C for 5 h. [73]

In another study, curcumin molecule, which is an anti-inflammatory and anti-tumorigenic molecule, was encapsulated into a hydrogel formed by self-assembling peptide (MAX8) in order to overcome the major drawbacks such as insolubility in water, low bioavailability and not being able to localize the curcumin delivery. *In vitro* studies with medulla blastoma cells revealed that encapsulation of curcumin within the hydrogel network did not influence its bioactivity and curcumin release can be controlled by changing concentration of peptide. [74]

1.5 Controlled Release from Peptide Gels

Hydrogels have been widely used as smart vehicles in controlled drug-delivery systems. There are many key parameters related to drug-delivery studies including (i) enhancing therapeutic efficacy and retention time of the drugs; (ii) reducing possible side effects of drugs; (iii) controlling release behavior; (iv) cost of therapy, (v) simple clinical application and administration.

To be able to understand molecular release mechanisms in hydrogels, a variety of models have been developed. These models are basically classified as (i) diffusion controlled; (ii) swelling-controlled, and (iii) chemically-controlled. Diffusion-controlled is the most appropriate mechanism for understanding drug release from hydrogels. In order to model the release, Fick's diffusion law is generally employed. [75]Drug diffusivity is mostly defined by using free volume, and hydrodynamic, or obstruction-based theories. Swelling-controlled release arises while the diffusion rate of drug is faster than hydrogel swelling. Drug release from hydroxypropyl methylcellulose (HPMC) hydrogel tablets is usually modelled with this route. For instance, Methocel networks which are mixtures of methylcellulose and HPMC are commercially available for swelling controlled drug release design with a wide range of delivery periods. [76–79] Chemically-controlled release based on molecular release comes from the reactions such as enzymatic degradation, or polymer chain cleavage happening within a delivery matrix. Commonly, degradation of hydrogel network will regulate the drug release properties. [80]

Self-assembled peptide nanofiber hydrogels are promising platforms for creating controlled drug delivery systems. Peptides can spontaneously assemble into highly ordered nanofibers with a stable secondary structure and form hydrogels under physiological conditions. Compared with the traditional polymer materials, they are more biocompatible, nontoxic, nonimmunogenic and tunable in terms of molecular design, and gelation behavior, and they can be functionalized according to the desired application. Also, their hydrophilic three-dimensional networks (99.5% w/v) may provide diffusion paths for various molecules.

The diversity of the amino acid sequence of these self-assembling peptides leads to controllable nanofiber properties at molecular level. This programmability may be advantageous for creating innovative delivery platforms as they provide diffusion of wide range of molecules. Tan and coworkers designed a drug delivery system by using self-assembling peptides RADAFI and RADAFII which contain the same amino acid compositions and different positions of one phenylalanine residue. These peptides show different physical morphology due to the alteration of $\prod$-$\prod$ stacking while they are self-assembling into nanofibrillar network. Also, they encapsulated different sized guest molecules such as phenylalanine (Phe), tryptophan (Trp), and phenol red (PR) into these hydrogel networks and observed release kinetics of these molecules according to Fickian diffusion model. Results showed that release properties were related to both the peptide design and the encapsulated molecules. The release from RADAFI was governed by the guest size while the guest lipophilicity controlled the release of RADAFII. [81]

Injectable and in situ-forming characteristics of hydrogels give them a remarkable potential as delivery vehicles for various hydrophobic drugs. Liu *et al*. have developed an injectable in situ gel drug delivery system based on mixture of self-assembling RADA16 peptide and paclitaxel (PTX) which is a hydrophobic antitumor drug. RADA16-PTX solution was able to form hydrogel under physiological conditions and exhibited extended toxic effect on growth of breast cancer cells in vitro. In the figure 1.4, it can be seen that the controlled release properties of the system are related to the hydrogel elasticity which is dependent on peptide concentrations. Higher peptide concentrations had prolonged drug release. Therefore, the volume of the hydrogel was significantly decreased during the 48

h release. [9] (Figure 1.9)

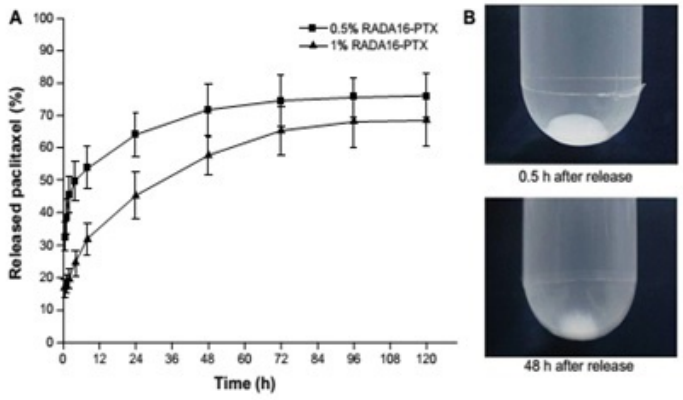

Figure 1.9: PTX release from RADA16-PTX hydrogel according to different concentrations of peptide in vitro. A) % release of drug from hydrogel during 120 h, b) hydrogel photographs which belongs to 30 min and 48 h after release (Reproduced from ref [9] with permission of 2011 Dove Medical Press).

1.6 Enzymatic Degradation of Peptide Gels

To entirely exploit a hydrogel in a biomedical framework, understanding of the degradation route is vital to design useful materials for desired applications. Degradation properties of a biomaterial give valuable information about the probable destiny in vivo. An understanding of the enzyme kinetics associated with these materials is important in order to design more resistant materials and prolong their life in the body.

Among the hydrogel materials, self-assembled peptide hydrogels have attracted considerable research attention because of their biological relevance. Recently, their applications for controlled drug release, which require that the hydrogels resist digestive enzymes and possess long term stability, have been studied extensively.

Recently, unnatural amino acids containing hydrogels have gained significant momentum thanks to their resistance to hydrolysis. They propose durable stability against the many proteolytic enzymes and show controlled release in vivo.

In one study, presence of D-amino acids in the peptide backbone dramatically enhanced the resistance of hydrogelator against proteinase K, which is a powerful proteolytic enzyme, however, still has its own limitations. For example, the extreme use of D-amino acids frequently causes immunogenic reactions and restricts their applications in vivo. [10](Figure 1.10)

There are many approaches for understanding degradation process of hydrogels in literature. Mazza *et al.* suggested two mechanisms for enzymatic interaction of peptide nanofibers with carboxipeptidase. [11]First mechanism proposes enzymatic degradation which is based on the separation of nanofiber integrity into smaller fragments. Enzyme attack at many spots breaks the H-bonds and disturbs the assembly into nanofibers. Broken H-bonds can cause more disordered packing as it enhances the molecular mobility. Hence, amino acids may be cleaved effortlessly due to less sterically hindered structure. The second mechanism offers enzymatic degradation, which causes a decrease in nanofibers length and generation of aggregates. (Figure 1.11)

To be able to verify that they incubated KRK peptide nanofibers in 0.05% trypsin EDTA, they visualized them by using TEM at different time intervals. After 30 minutes of incubation, nanofibers were stable and protected their structural integrity. There was a decrease in nanofiber length after 24 h of incubation. At day 14, peptide nanofibers were hardly observed by TEM. Also, they incubated peptide nanofibers with cell culture medium (MEM) which has no enzyme. Results showed that there was no significant degradation in MEM except for the eventual aggregation due to the buffering effect. (Figure 1.12) They concluded that enzymatic degradation of peptide nanofibers prefers the second mechanism due to the significant reduction in nanofiber length and structural degradation.

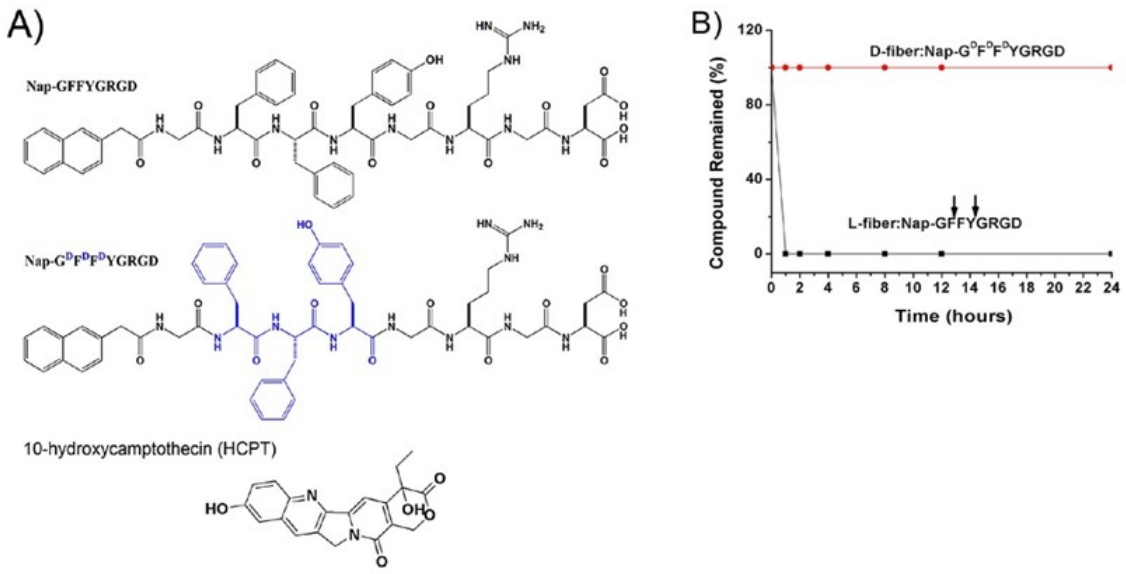

Figure 1.10: 10-Hydroxycamptothecin release from D-amino acids containing nanofibers (a) Chemical Structures of Nap-GFFYGRGD, Nap-GDFDFD YGRGD, and 10-hydroxycamptothecin (HCPT); b) stability of L-fiber and D-fiber against proteinase K digestion in PBS buffer solution (pH 7.4) (Reproduced from ref [10] with permission of 2014 American Chemical Society).

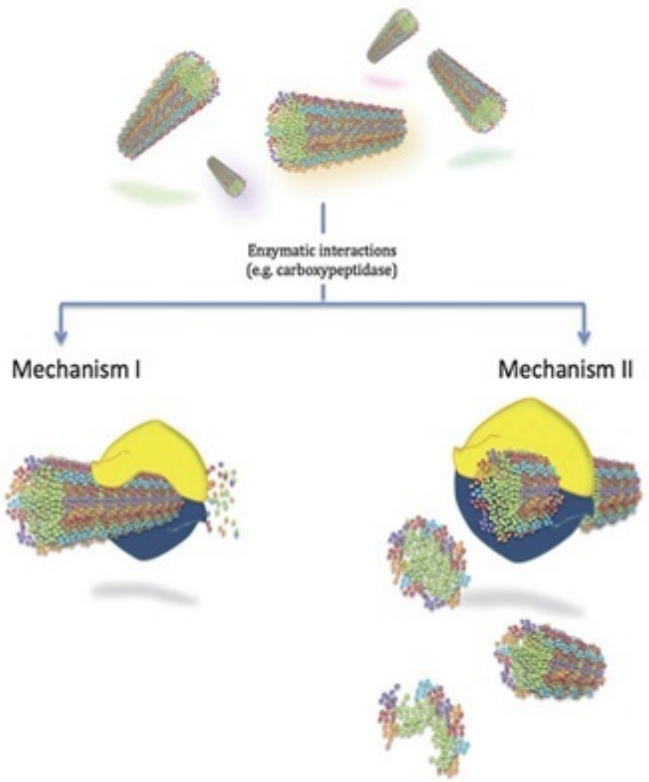

Figure 1.11: Illustration of projected degradation behaviors of PNF degradation. (Reproduced from Ref [11] with permission of The Royal Society of Chemistry).

In a different study, Hartgerink and coworkers demonstrated that the MMP-2 specific cleavage site containing peptide nanofiber gels were utterly degraded with collagenase IV in HEPES-buffered saline solution after one month. In order to analyze the degradation behavior, weight loss method and TEM imaging were employed (Figure 1.12) Findings indicated that the peptide nanofiber gels lost 50% of their weight in the presence of collagenase IV in one week. [82]

After three weeks, the nanofibers lost their uniform structure and transformed to egg shaped aggregates or twisted ribbons. The interesting point of this study was that there was no instant breaking of the fiber into two pieces at the enzyme specific cleavage site. In place of that, enzyme generates defects in the fiber packaging. Increasing the number of the defects changed the favored packing from cylindrical structures to smaller, non-uniform fragments, which were visualized by TEM.

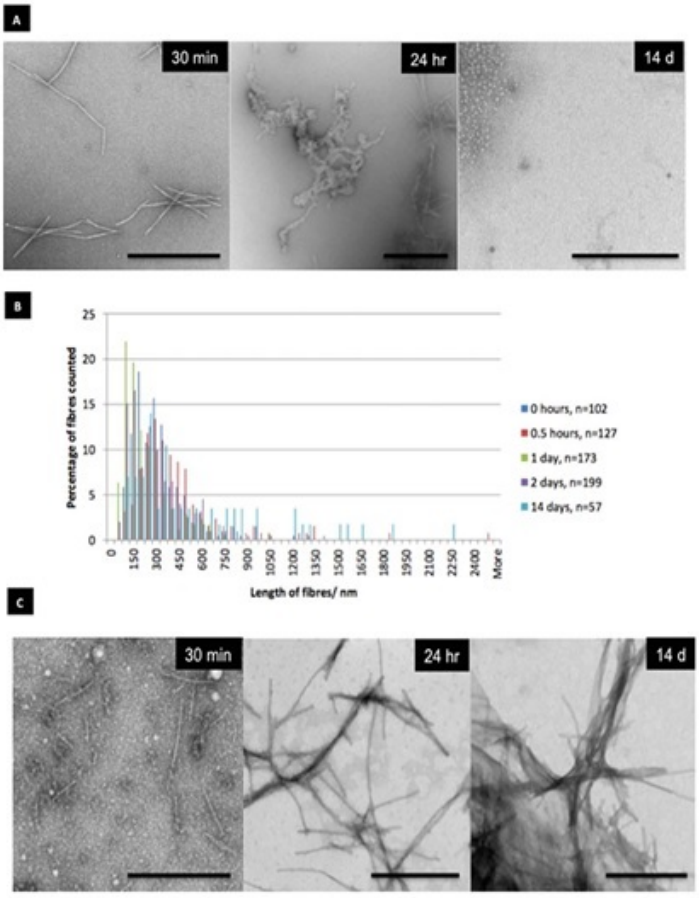

Figure 1.12: Observation of degradation of peptide nanofibers by TEM a) TEM images of peptide nanofibers which is incubated with 0.5% trypsin-EDTA, b) Image J analysis of length of nanofibers, c) TEM images of peptide nanofibers which are incubated with cell culture media (Reproduced from ref [11] with permission of The Royal Society of Chemistry).

Chapter 2

Enzymatic Degradation of Self-Assembled Peptide Nanofiber Gels

2.1 Introduction

Peptide amphiphiles (PAs) constitute important class of self-assembled peptides. They consist of four segments: (i) long alkyl tail which promotes hydrophobic collapse; (ii) β-sheet forming sequence for generation of hydrogen bonding, (iii) charged groups in order to provide solubility, electrostatic intractions, reactions etc. and (iv) bioactive epitopes. They can self-assemble into highly ordered hierarchical nanostructures such as nanofibers, nanotubes and nanospheres as a result of pH change, concentration (monomer amount), salt addition or ionic strength. [83–85] The self-assembly of PA molecules allows the formation of high-aspect-ratio nanofibers, which can then arrange themselves into three-dimensional networks to generate gel matrices.

Recently, peptide based supramolecular gels, which are composed of L-amino acid sequences have received extensive interest for various biomedical applications such as tissue engineering scaffolds, drug delivery vehicles and wound healing covering and biomineralization matrices. They display many advantages such as biocompatibility, biodegradability and easy functionalization for specific purposes. In order to use these peptide based gels effectively in in vivo applications, these matrices should be stable against the enzymatic degradation during treatment. However, some studies revealed that small peptide-based hydrogelators may show inherent susceptibility to proteolytic degradation and this leads to faster degradation and shortened *in vivo* half life time. For example, in vivo stability of Nap-FFY hydrogels is shorter than 24 h. [86]

Current endeavors have focused to design and synthesize new types of peptide based molecules in order to promote prolonged biostability, bioavailability and biofunctionality. The use of unnatural amino acids such as D-amino acids for rational peptide design and engineering have became more attractive. [86] Li *et al*. integrated D-amino acids into peptide backbone to enhance the stability of peptide derivatives towards the enzymatic degradation. According to the results, D-amino acids containing hydrogelators exhibited increased biostability against proteinase K after 24 h of incubation. However, rheological analysis revealed that

the presence of D-amino acids on the peptide backbone probably reduces the intermolecular interactions by changing the peptide conformation and disrupts the self-assembly. [87] In addition; it is noteworthy that the excessive use of unnatural amino acids causes immunogenic response frequently and obstructs *in vivo* applications.

In a comprehensive study, researchers determined *in vivo* stability, biodistribution and toxicity of self-assembling L-fibers (NapGFFYGRGD), and D-fibers (Nap$G^{D}F^{D}F^{D}$YGRGD). The results exhibited that the D-fibers are more stable than L-fibers *in vitro* and *in vivo*. While L-fibers were completely degraded in plasma during 6 h, D-fibers preserved their overall structure in plasma for the period of 24 h. Biodistrubution studies revealed that the L-fibers mostly accumulate in stomach, while D-fibers prefer liver for accumulation. In a pioneering study, D-amino acids containing dipeptide hydrogelators were also used for controlled drug release applications in vivo. [88]

In this work, we visualized the proteolytic stability of D-E_3/K_3PA, L- E_3/K_3PA and DL- E_3/K_3PA nanofibers in the presence of proteinase K for 14 days with the help of TEM. Then, we determined the degradation percentage of peptide gels in both enzyme and no enzyme containing buffer solution by the weight loss method during 29 days. Finally, we investigated the connection between the degradation behavior and bulk release properties by measuring the absorbance of Rhodamine B dye, which was released from the PA gels with UV-Vis spectroscopy. This study will be helpful to understand the link between molecular structure and bulk release mechanism, for developing smart drug delivery systems.

2.2 Experimental Section

2.2.1 Materials

9-Fluorenylmethoxycarbonyl (Fmoc) and other protected amino acids, lauric acid, [4-[α-(2,4-dimethoxyphenyl) Fmoc-amino methyl]phenoxy] acetomidonorleucyl-MBHA resin (Rink amide MBHA resin), and 2-(1H-Benzotriazol-1-yl)-1,1,3,3-tetramethyluronium hexafluorophosphate (HBTU), were purchased from NovaBiochem. All solvents were purchased from Sigma Aldrich.

2.2.2 Synthesis of Peptide Amphiphiles

Standard Fmoc solid phase peptide synthesis method was used to synthesize D-Lauryl-Val-Val-Ala-Gly-Glu-Glu-Glu-OH (D-E_3PA), L-Lauryl-Val-Val-Ala-Gly-Glu-Glu-Glu-OH (L-E_3PA) and D-Lauryl-Val-Val-Val-Ala-Gly-Lys-Lys-Lys-Am (D-K_3PA), L-Lauryl-Val-Val-Val-Ala-Gly-Lys-Lys-Lys-Am. D-K_3PA and L-K_3PA were constructed on MBHA Rink Amide resin; D-E_3PA and L-E_3PA were constructed on Fmoc Glu(OtBu)-Wang resin. Amino acid couplings were performed with 2 equivalents of Fmoc-protected amino acid, 1.95 equivalents of HBTU and 3 equivalents of N,N-diisopropylethylamine (DIEA) and then the mixture was shaken for at least 2 hours. In order to remove the Fmoc group, 20% (v/v) piperidine/ N,N-Dimethylmethanamide (DMF) solution was used during a 20 min incubation period. 10% (v/v) acetic anhydride solution in DMF was used for blocking the remaining free amine groups after coupling for 30 min. After each step, the resin was washed with DMF, dichloromethane (DCM), and DMF (three times each). The PAs were cleaved from the resin by using TFA/TIS/H2O mixture (95:2.5:2.5 ratio) for 2 h. The excess TFA was removed by applying rotary evaporation method. The remaining of the peptide solution was dispersed in diethyl ether and left for overnight incubation at -20°C. Then, the peptides were removed from diethyl ether by centrifugation. After the drying session, the resulting white precipitate was dissolved in double distilled water and then

freeze-dried. (Table 2.1)

2.2.3 Characterizations of Synthesized Peptide Amphiphiles

2.2.3.1 Liquid Chromatography Mass Spectrometry (LC-MS)

1 mL of water was used to dissolve 1 mg of the peptides, then the solutions were sonicated for 15 min. LC-MS measurements were taken with Agilent Technologies 6530 Accurate-Mass QTOF system equipped with a Zorbox Extend-C18 column. 0.1% (v/v) ammonium hydroxide water (A) and 0.1% (v/v) ammonium hydroxide acetonitrile (B) were used as mobile phase for the analysis of the negatively charged peptides (D-E3PA and L-E3PA); 0.1% formic acid-water (A) and 1% formic acid- acetonitrile (B) were used as a mobile phase for the positively charged peptides (D-K3PA and L-K3PA). The flow rate of mobile phase was 0.65 mL/min. For the first 2 min, flow composition was 98% A 2% B, then B increased to 98% between 2nd and 25th min and then turned back to 2% for the next two minutes. LC chromatogram was obtained at 220 nm.

2.2.3.2 Preparative High Performance Liquid Chromatography (Prep-HPLC)

An Agilent 1200 preparative reverse-phase HPLC system was used to purify the peptides. The mobile phase for the negatively charged peptides (D-E_3PA and L-E_3PA) were 0.1% (v/v) ammonium hydroxide water (A) solution and 0.1% (v/v) ammonium hydroxide acetonitrile (B) solution; for the positively charged peptides ((D-K_3PA and L-K_3PA), it was 0.1% (v/v) trifluoroacetic acid (TFA) water (A) solution and 0.1% (v/v) trifluoroacetic acid (TFA) acetonitrile (B).

Table 2.1: peptide amphiphile molecules (*theoretical net charge at pH 7.4)

PA sequence	Nomenclature	Net charge
Lauryl-VVAGKKK	L-K_3PA	+3
Lauryl-vvaGkkk	D-K_3PA	+3
Lauryl-VVAGEEE	L-E_3PA	-4
Lauryl-vvaGeee	D-E_3PA	-4

2.2.3.3 Circular Dichroism (CD)

The secondary structure of peptide nanofibers were investigated by JASCO J815 CD spectrometer. Crude peptides were dissolved in double distilled water and sonicated to obtain a homogeneous solution as 1% (w/v). Final peptide solution concentrations were 10.94 mM for D-and L-E_3PA and 10.98 mM for D- and L-K_3PA. Oppositely charged peptide solutions were neutralized by mixin at 4:3 (D:L) ratio to form self-assembled peptide nanofiber gels through the electrostatic interactions at neutral pH. In order to prepare 100 L of D- E_3/K_3 gel: 57 L D-K_3PA and 43 L D-E_3PA ; for L- E_3/K_3 gel: 57 L L-K_3PA and 43 L L-E3PA; and for DL- E_3/K_3 gel: 28.5 L D-K_3PA, 28.5 L L-K_3PA, 21.5 L D-E_3PA, 21.5 L L-E_3PA solutions were mixed and left for overnight incubation. (Table 2.2) Peptide gels were diluted 30 times without sonication to form final concentrations of 0.033% (w/v). 300L of the diluted PA gel solutions were put into 1 mm thick quartz cells and measured from 300 nm to 190 nm, with data interval and data pitch of 0.1 nm, scanning speed of 100 nm/min, and three times of accumulations. The digital integration time (DIT) was selected as 1 s, the bandwidth as 1 nm, and the sensitivity as standard sensitivity. The measurements were taken at room temperature.

Table 2.2: Nomenclature and compositions of the PA gels

Nomenclature	Gel/nanofiber compositon	Volume mixing ratio
D-E_3/K_3	D-E_3PA/D-K_3PA	3:4
L-E_3/K_3	L-E_3PA/L-K_3PA	3:4
DL-E_3/K_3	DL-E_3PA/DL-K_3PA	3:4

2.2.3.4 Oscillatory Rheology

Rheology measurements were performed with an Anton Paar Physica RM301 Rheometer equipped with a 25 mm parallel plate at 25°C. Previously prepared 1% (w/v) oppositely charged peptide solutions were mixed as with 250 μL total volume. Measuring distance was determined as 0.5 mm. Gelation kinetics of the gels was investigated with time-sweep test. During the test, angular frequency was 10 rad s^{-1} and strain was 0.01%. Amplitude sweep test was performed with increasing strain amplitude from 0.01 to 1000% at constant angular frequency (10 rad s^{-1}.

2.2.3.5 TEM Imaging

A FEI Tecnai G2F30 TEM instrument was used to visualize resulting nanostructures of diluted gel samples. Briefly, overnight incubated 1% (w/v) PA gels were diluted in 1:30 ratio by addition of double distilled water. 10 μL of diluted gel samples were dropped onto TEM grid and waited for 10 min. After that, excess sample solution was separated from grid surface by micropipeting. 2% (w/v) uranyl acetate which is a negative stain was casted onto grid and waited for 5 min. Then, excess uranyl acetate was removed and the grid was left to dry.

2.2.3.6 SEM Imaging

To visualize 3D nanofiber network formation of self-assembled PA gels, scanning electron microscopy (SEM) was performed. 1% (w/v) PA gels were prepared on cleaned silicon wafer surfaces. Then, they were dehydrated in 20%, 40%, 60%, 80% and 100% ethanol solutions, respectively. The dehydrated PA nanofiber gels were dried with a Tourismis Autosamdri-815B critical-point-drier to maintain the 3D network arrangement. Samples were coated with 6 nm gold/palladium prior to imaging. A FEI Quanta 200 FEG scanning electron microscope was employed to image gel networks.

2.2.4 Weight Based Degradation of Self-Assembled Peptide Gels

In order to determine degradation behavior of D-E_3/K_3, L-E_3/K_3 and DL-E_3/K_3, the gels were prepared as described above. First, empty glass vials were weighted and then 300 μL of the gels were made. After 3 h passed from the attained equilibrium of the gels, their weights were measured. Then, prepared gels were separated into two groups, which were then incubated with (i) 900 μL Proteinase K solution at 1mg/mL in Tris buffer or Tris Buffer as a control. (n=3) The sample solutions were changed at definite time intervals including day 2, day 4, day 8, day 15, day 22 and day 29.

2.2.5 Degradation of Self-Assembled Peptide Nanofibers

1 mg of each peptide amphiphile molecule was dissolved in 100 μL double distilled water and sonicated to obtain homogenous peptide solutions with concentration of 1% (w/v). Then, the oppositely charged peptide amphiphile molecules were mixed to form self-assembled peptide gels and left for overnight incubation. In order to get peptide nanofiber solutions with concentration of 0.1% (w/v), the prepared gels were diluted 1:10 ratio. After that, 100 μL of peptide nanofiber

solutions were mixed with 900 μL Tris buffer or proteinase K solution (1 mg/mL). TEM imaging was done at defined time intervals including 0 h, 24 h, 48 h, day 7, and day 14.

2.2.6 Rhodamine B release from self-assembled peptide gels

In the release studies, 1 mg of each peptide amphiphile molecule was dissolved in 100 μL double distilled water to form peptide solutions at a concentration of 1% (w/v). For D-E_3/K_3 and L-E_3/K_3 gels, 1% (w/v) K_3PA solution (160 μL) was mixed with 750 μM Rhodamine B (20 μL) and then the oppositely charged 1% (w/v) E_3PA solution (120 μL) was added on to the K_3PA-Rhodamine B mixture to form self-assembled peptide gel. In the case of DL-E_3/K_3 gels, 1% (w/v) D-K_3PA (80 μL) and L-K_3PA (80 μL) solutions; 1% (w/v) D-E_3PA (60 μL) and L-E_3PA (60 μL) solutions were mixed separately, vortexed and sonicated for 15 min. Then, 160 μL of D- and L- mixture of K_3PAs were blended with 750 μM Rhodamine B (20 μL) and then D- and L- mixture of E_3PA solution (120 μL) was added to promote gelation. (Figure 2.1) The samples were prepared in quartz cuvettes and left for 3 h of incubation to attain equilibrium of the gels. Furthermore, 2.2 mL Proteinase K solution (1 mg/mL) or Tris Buffer solution (10mM) as control was added on top of the gels (n=3). Absorbance of the solutions were measured between 400 and 600 nm with Varian Cary 100 UV-Vis spectrophotometer at definite time intervals including 0 h, 2 h, 8 h, 12 h, 24 h, 48 h, 72 h, 96 h at room temperature. (Figure 2.1)

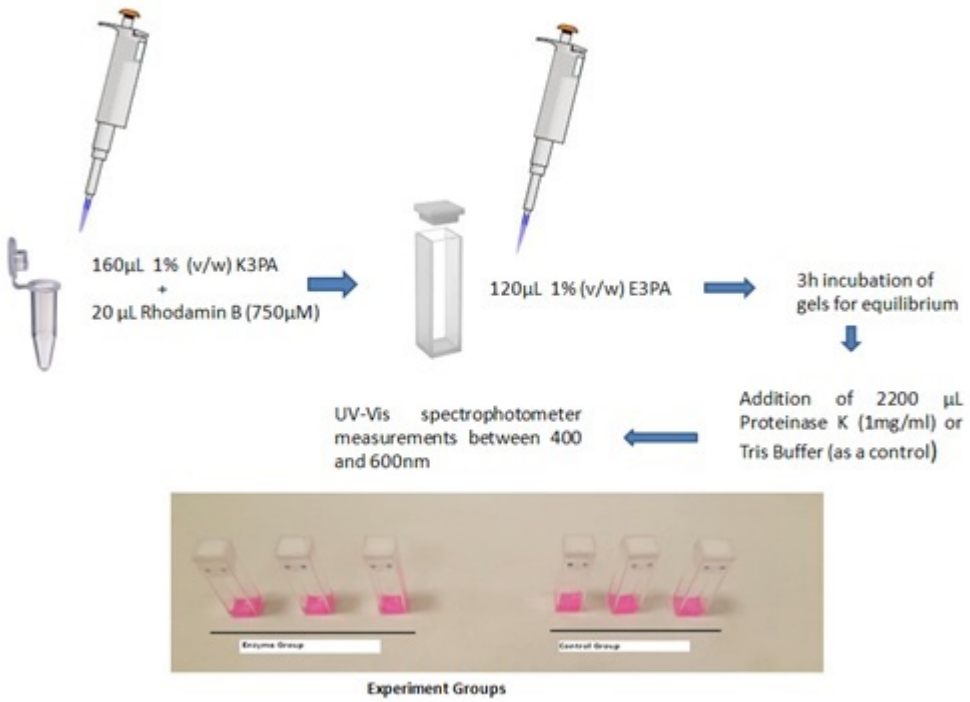

Figure 2.1: Schematic illustration of Rhodamine B release experimental setup

2.3 Results and Discussion

In this work, four different peptide amphiphile molecules, L-form Lauryl-VVAGEKKK-Am [L-K_3PA], D-form Lauryl-VVAGEKKK-Am [D-K_3PA], L-form Lauryl-VVAGEEE-OH [L-E_3PA], D-form Lauryl-VVAGEEE-OH [D-E_3PA] were designed and synthesized according to Fmoc-SPPS approach and followed by alkylation with lauric acid. Designed peptides are composed of three major segments: (i) a hydrophobic alkyl group, (ii) β-sheet forming sequence, (iii) and charged groups. Lauric acid is used as hydrophobic alkyl tail to promote aggregation. The second segment (VVA) which is adjacent to alkyl tail is the β-sheet forming sequence. This region has the hydrophobic amino acids which have great propensity to form intermolecular hydrogen bonding, which generally ends up forming β-sheets. The last region is the charged groups (positively charged, KKK; and negatively charged EEE) which is responsible for solubility of the peptides in water.

Basically, the negatively charged E_3PA and the positively charged K_3PA molecules were mixed in order to achieve self-assembled peptide amhiphile nanofibers which are driven by electrostatic interactions at physiological pH. These nanofiber structures in the aqueous media transform into three dimensional PA gel network. (Figure 2.2)

The peptide amphiphile molecules were purified using Prep-HPLC after the synthesis to separate the unintended materials from the mentioned peptides. The purified peptide amphiphiles were dissolved in double distilled water with concentration of 1 mg/mL and then analyzed by using Q-TOF LC-MS to determine the final purity and the molecular weight of the peptides.

The chromatograms showed that the purity of both peptides were more than 95%. (Figure 2.3-6) According to the mass spectra results, the molecular weights of E_3PA and K_3PA were found as 912 g/mol and 914 g/mol, respectively, which were nearly the same with the calculated mass.

Circular dichroism (CD) spectroscopy was used for determination of the secondary structures and the chiral conformations of the designed PAs. This technique relies on the absorbance differences between right-handed polarized light and left-handed polarized light which comes from the molecule chirality in the far-UV region. CD spectra of the samples were red-shifted relative to typical β-sheets with a maximum at 195 nm and a minimum at 216 nm at neutral pH. The red-shifted β-sheet signals are associated with a twisted structure. 50% mixture of these chiral molecules decreased the intensity. This could be due to batch to batch variation in synthesis causing variable TFA content. TFA molecules which did not separate from lysine residues of the L- and D- K_3PA may have role in this difference. (Figure 2.7)

TEM imaging was employed to visualize the nanofibers and the network properties. It revealed that the co-assembly of the oppositely charged peptide amphiphiles self-assemble into high-aspect-ratio nanofiber structures with diameters of about 6-10 nm and lengths in terms of micrometers. (Figure 2.8)

SEM imaging was also performed to observe 3D network of self-assembled PA gels. Resulting images indicated that D-E_3/K_3, L-E_3/K_3 and DL- E_3/K_3 gel networks have similar nanofiber network. (Figure 2.9)

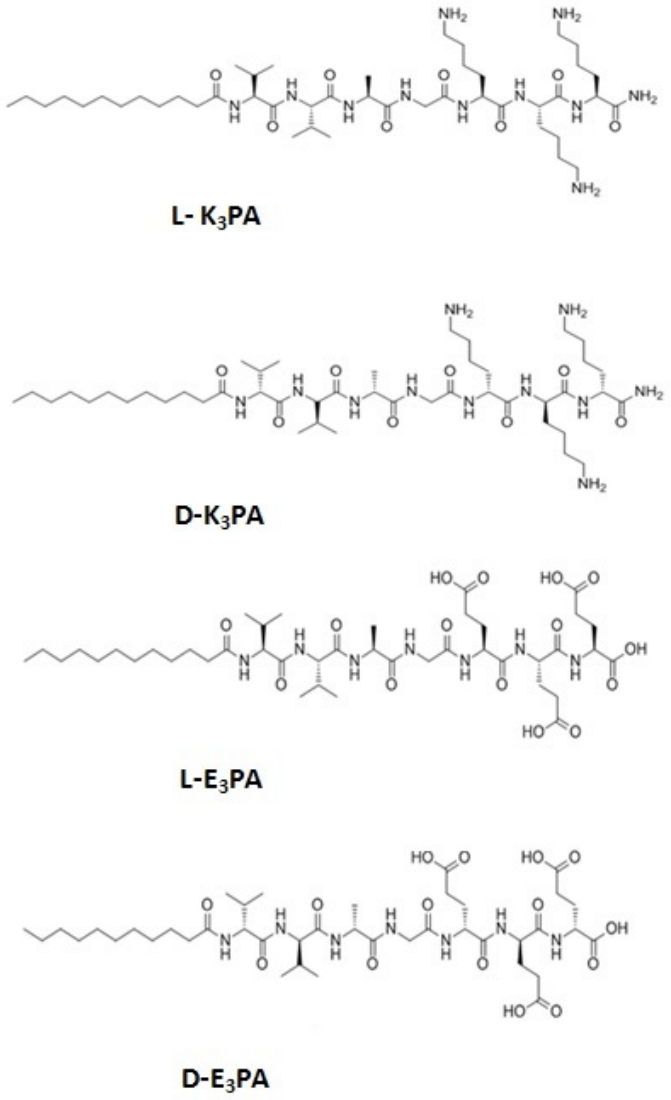

Figure 2.2: Chemical structures of peptide amphiphiles (a) L-K_3PA, (b) D-K_3PA, (c) L-E_3PA, and (d) D-E_3PA

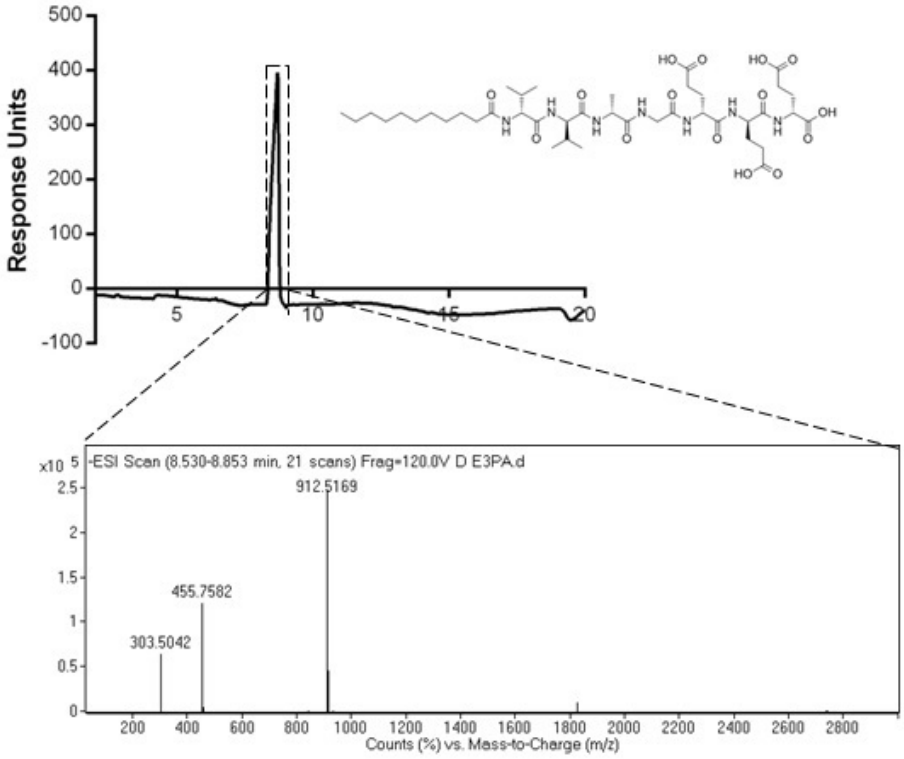

Figure 2.3: Characterization of D-E_3PA by using LC-MS. Liquid chromatogram of D-E_3PA by the absorbance at 220 nm (top). mass spectrum of D-E_3PA (bottom). MS: (m/z) calculated 914.05, $[M\text{-}H]^-$ observed 912.5169, $[M\text{-}2H]^-/2$ observed 455.7582, $[M\text{-}3H]^-/3$ observed 303.5042

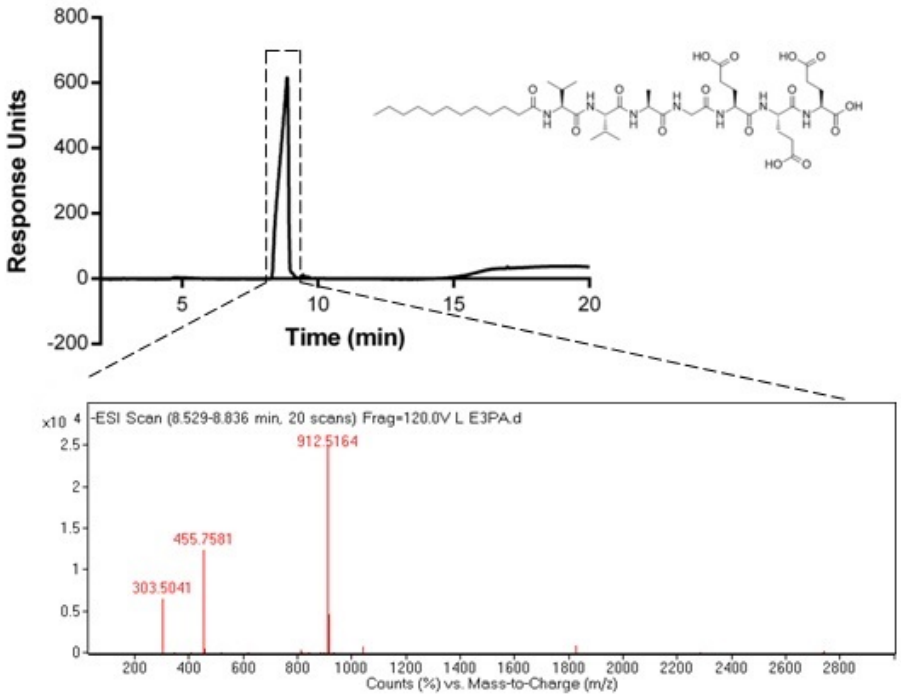

Figure 2.4: Characterization of L-E_3PA by using LC-MS. Liquid chromatogram of L-E_3PA by the absorbance at 220 nm (top), Mass Spectrum of E_3PA (bottom). MS: (m/z) calculated 914.05, $[M-H]^-$ observed 912.5164, $[M-2H]^-/2$ observed 455.7581, $[M-3H]^-/3$ observed 303.5041

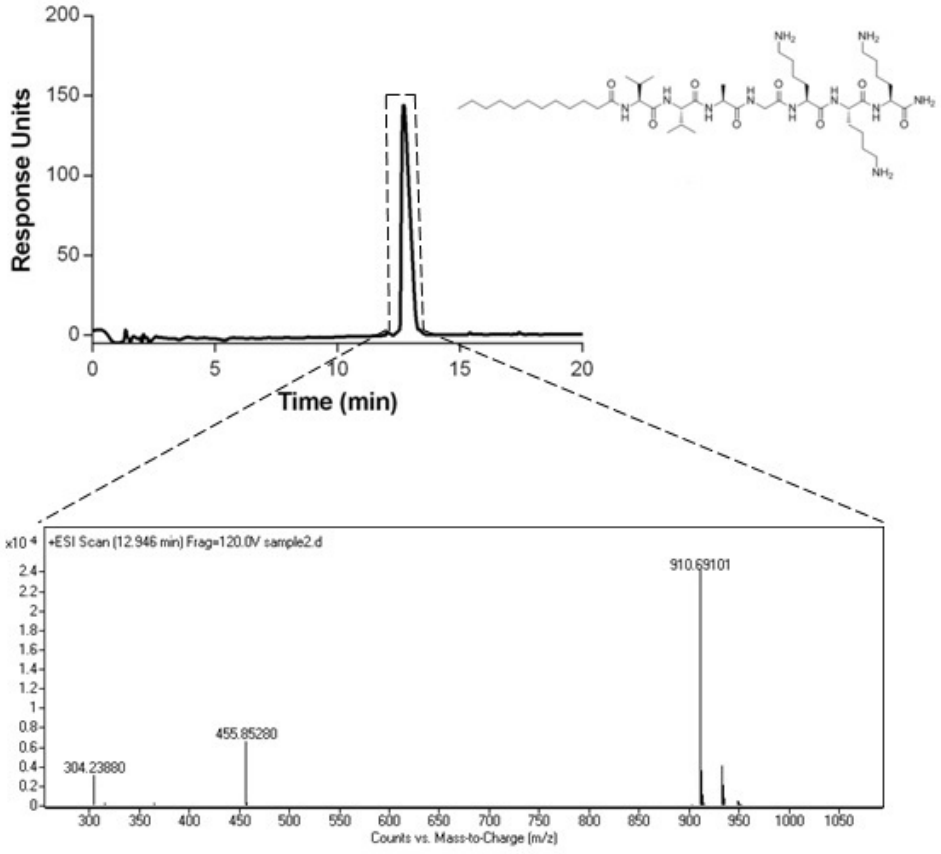

Figure 2.5: Characterization of L-K_3PA by using LC-MS. Liquid chromatogram of L-K_3PA by the absorbance at 220 nm (top). mass spectrum of K_3PA (bottom). MS: (m/z) calculated 910.24, $[M+H]^+$ observed 910.4739 $[M+2H]^+/2$ observed 455.6983 $[M+3H]^+/3$ observed 304.1126

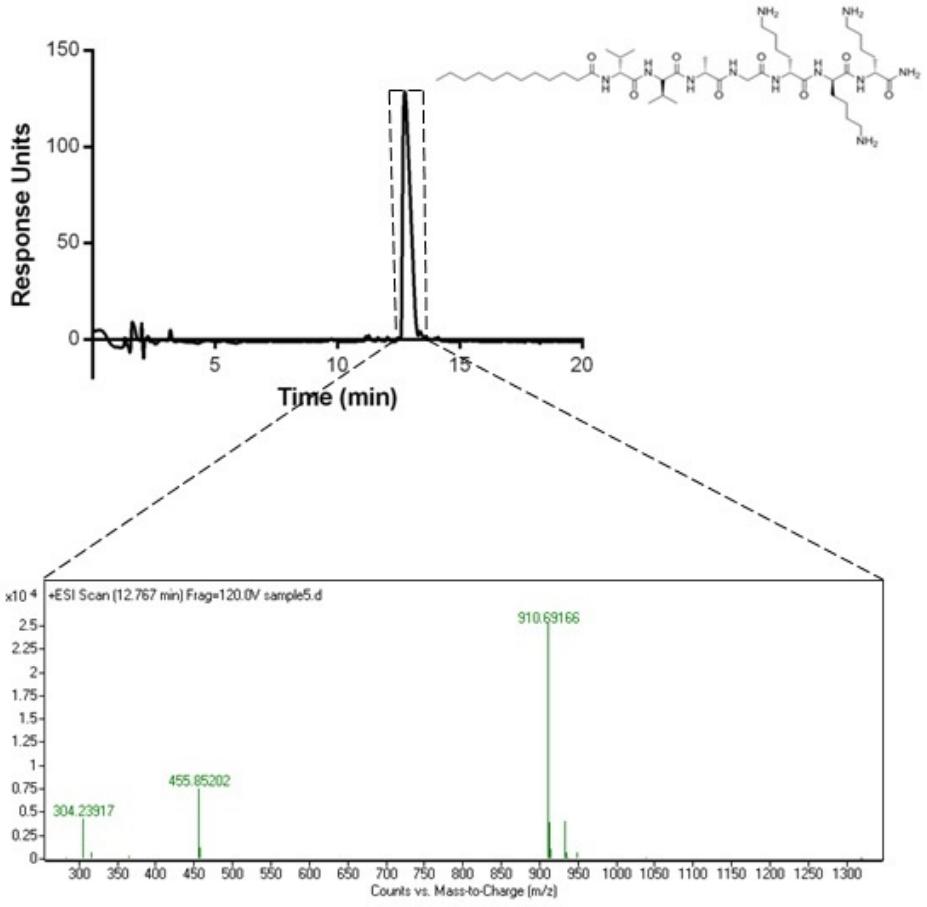

Figure 2.6: Characterization of D-K_3PA by using LC-MS. Liquid chromatogram of D-K_3PA by the absorbance at 220 nm (top). mass spectrum of K_3PA (bottom). MS: (m/z) calculated 910.24, $[M+H]^+$ observed 910.69166, $[M+2H]^+/2$ observed 455.85202, $[M+3H]^+/3$ observed 304.23917

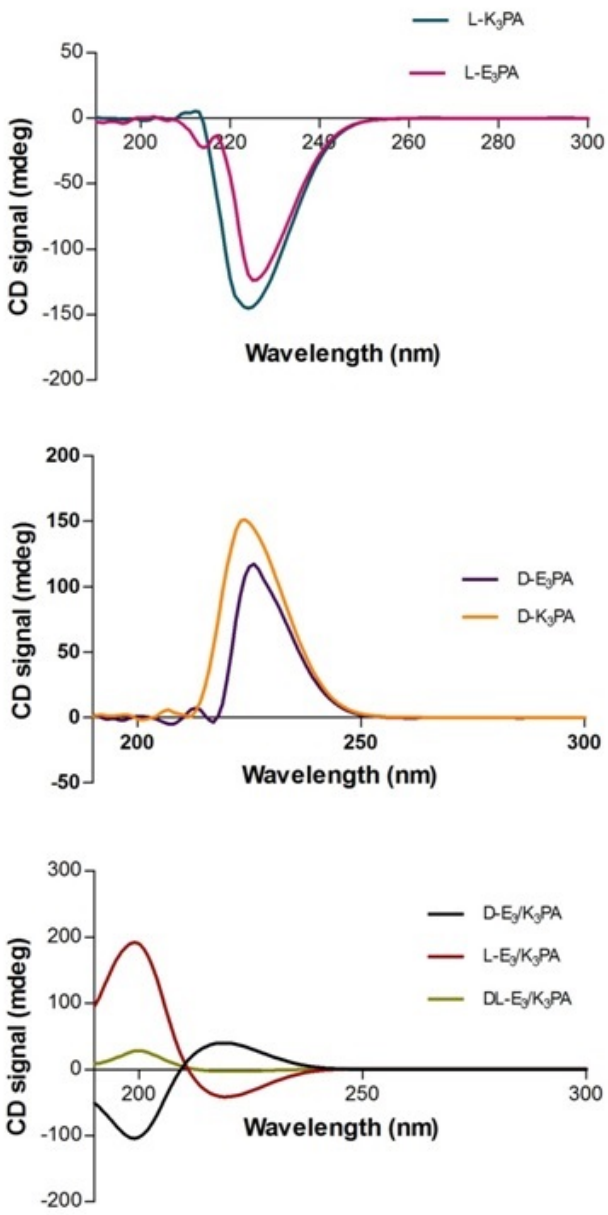

Figure 2.7: Circular dichroism spectra of synthesized peptide amphiphiles

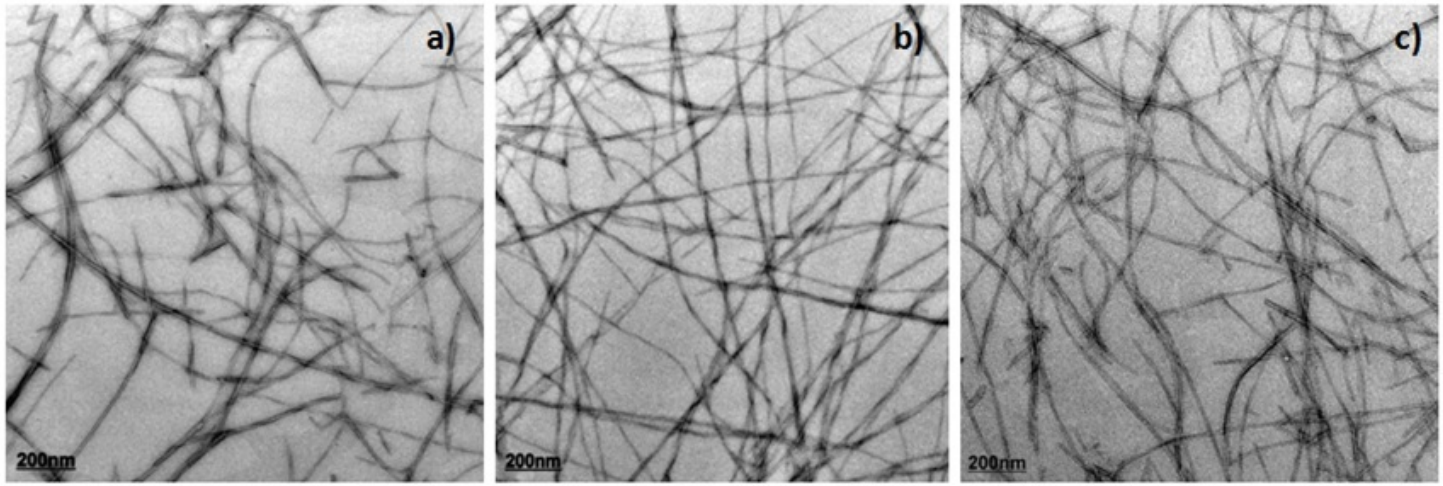

Figure 2.8: TEM images of peptide amphiphile gels a) D-E_3/K_3 stained with uranyl acetate, (b) L-E_3/K_3 stained with uranyl acetate, (c) DL -E_3/K_3 stained with uranyl acetate

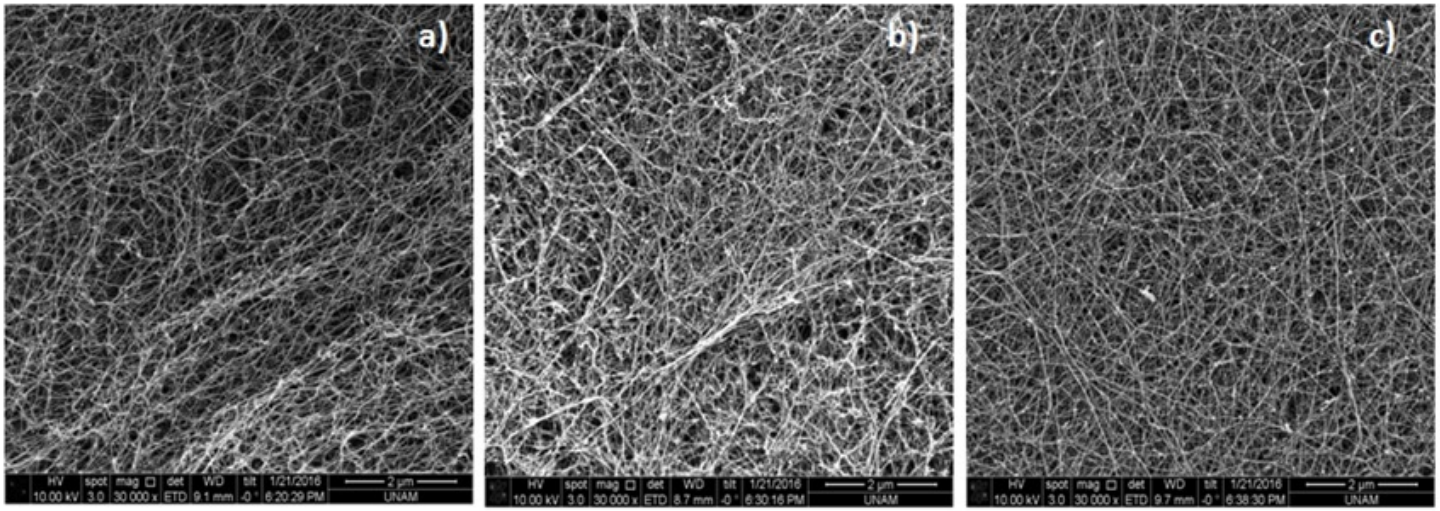

Figure 2.9: SEM imaging of peptide amphiphile gels a) 1% (w/v) D-E_3/K_3; (b) 1% (w/v) L-E_3/K_3; (c) 1% (w/v) DL-E_3/K_3

par After the synthesis and characterizations of the peptide amphiphile molecules, gel formation properties were investigated. The D-K_3PA and the L-K_3PA had good solubility in water and their final pH values were around 5. Solubilities of the D-, and the L- E_3PA in water were enhanced by adding NaOH (1 M) into the peptide solutions and their final pH values were around 7.4. When the oppositely charged PAs were mixed, they formed milky white gels which can be observed by naked eye. (Figure 2.10) These three-dimensional networks contain extended nanofibers which can bundle up and trap the water molecules inside and result in gel formation.

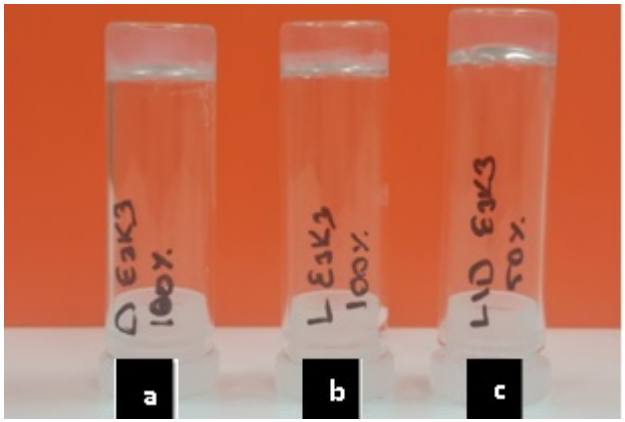

Figure 2.10: Photograph of the gels of (a) D-E_3/K_3 (1.0 wt%, pH 7.4); (b) L-E_3/K_3 (1.0 wt%, pH 7.4); (c) DL-E_3/K_3 (1.0 wt%, pH 7.4)

The mechanical strength and viscoelastic properties of these gel matrices were evaluated by oscillatory rheology measurements. Gelation kinetic was monitored by a time-sweep test within the linear viscoelastic region. Storage modulus (G) of the gels reached a stable plateau which reveals the complete gelation was finished within 30 min. However, the DL-$E_3/_3$ gels took much longer to reach stationary phase compared with the other gels. This result may indicate that the self-assembly process is much more complicated due to the mixture of the different chiral molecules. On the other hand, the required times to reach the plateaus were almost the same for the D-E_3/K_3PA and the L-E_3/K_3PA gels. The results also exhibited that the storage modulus (G) of all the gel groups are notably higher than their loss modul (G), suggesting a solid-like rheological behavior and proving the gel formation during the self-assembly process. The D-E_3/K_3PA had slightly higher storage modulus compared with the L-E_3/K_3PA. The DL-E_3/K_3PA had the highest storage modulus. It was approximately five times higher than the storage moduli of the L-E_3/K_3PA gels, and three times higher than the storage moduli of the D-E_3/K_3PA gels. (Figure 2.11) Having resemblance in the TEM image of the gel networks also indicated that the enhanced rigidity in the DL-E_3/K_3PA gel is not related with the nanofiber morphology. This phenomenon might be explained by the energetically favorable chiral relationship between the peptide molecules. It may suggest that chirality can be a useful property to adjust the mechanical rigidity of the self-assembled systems.

In order to investigate the viscoelastic properties of the PA gels, amplitude sweep test was employed. According to the results, increasing strain values did not change the storage modulus of the gels within linear viscoelastic region. After exceeding the limiting strain amplitude (LSA), the storage modulus of the gels started to decrease while the employed strain was still increasing. This represents the transition from linear to nonlinear viscoelastic behavior. (Figure 2.11)

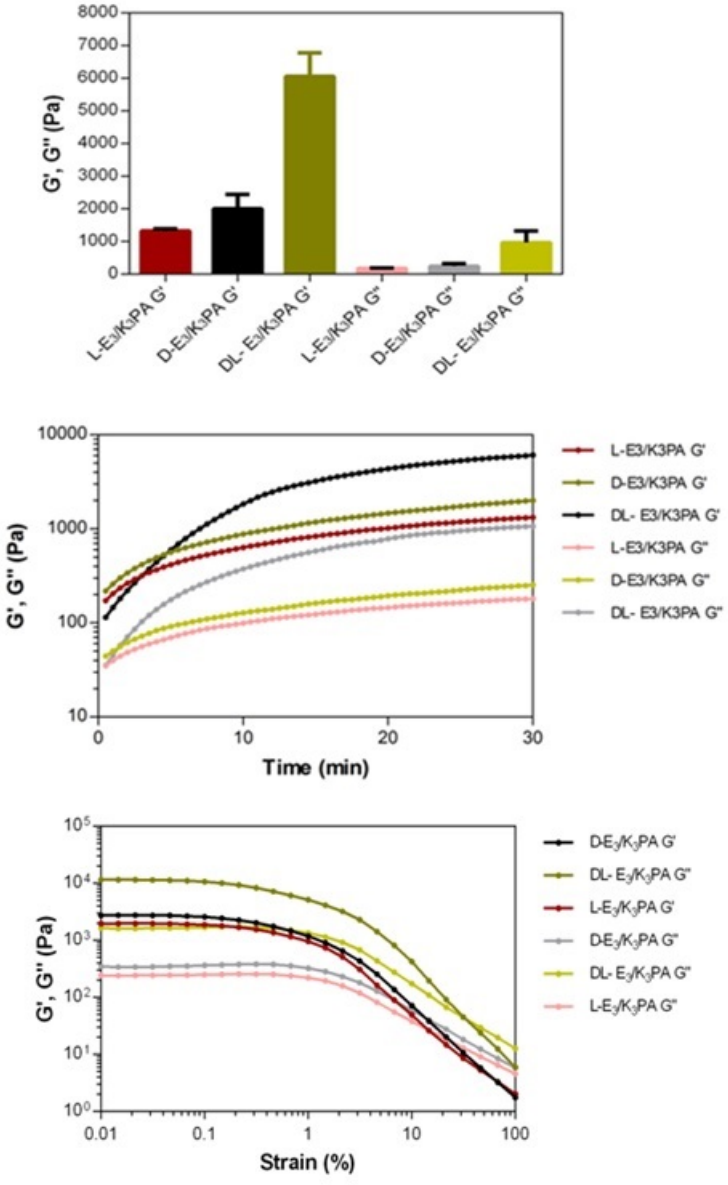

Figure 2.11: Rheology results of self-assembled peptide gels. Time sweep test (top), Amplitude sweep test (bottom)

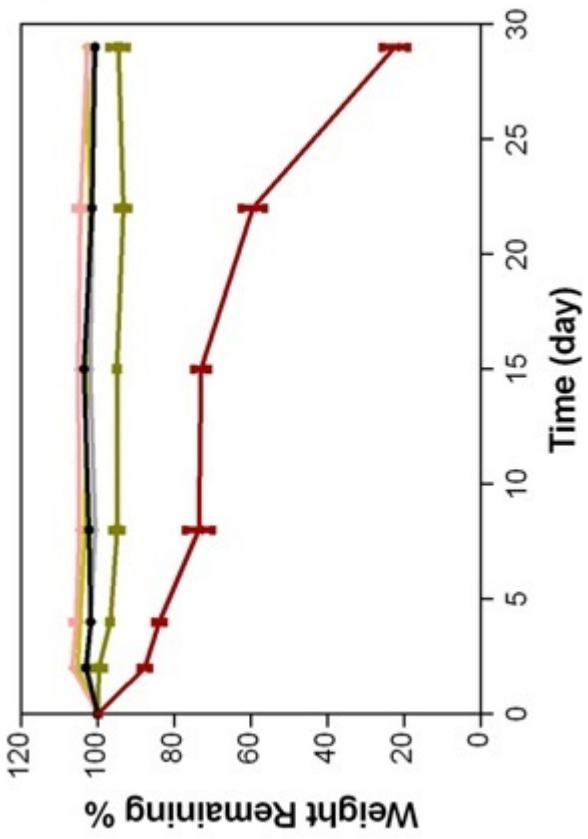

Figure 2.12: Weight based enzymatic degradation of peptide amphiphile gels

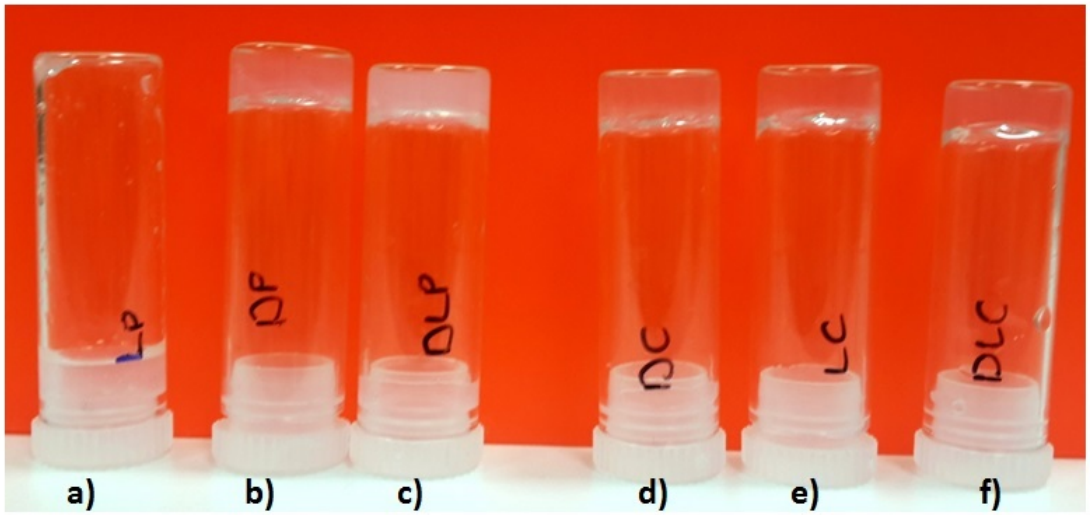

Figure 2.13: Photograph of self-assembled peptide nanofiber gel degradation after 29 day incubation with proteinase K. (a) L-E_3/K_3 incubated with proteinase K; (b) D-E_3/K_3 incubated with proteinase K; (c) DL-E_3/K_3 incubated with proteinase K; (d) D-E_3/K_3 incubated with Tris buffer; (e) L-E_3/K_3 incubated with Tris buffer ; (f) DL-E_3/K_3 incubated with Tris buffer

To use the peptide amphiphile gels for possible in vivo applications, we determined the proteolytic degradation profiles of these different gel networks by using weight loss method. (Figure 2.12-13) Briefly, the PA gels (1 wt%, 300 μL) were prepared by mixing the oppositely charged E_3PA and K_3PA molecules as described above after weighing the empty tubes. After 3 h from the equilibration, the samples were separated into two groups and then incubated with 2200 μL of proteinase K (1 mg/mL) or Tris buffer as a control, and then stored at room temperature. The sample solutions were changed and the remaining gels were weighed at determined time intervals. It was found that these gels display varying susceptibilities to the protease degradation. Even after several days of incubation, the D-E_3/K_3 and the DL-E_3K_3 gels showed only minimal loss of the gel integrity compared to the L-E_3/K_3. At 29 days of incubation, the L-E_3/K_3 gels lost approximately 80% of their weight in the presence of the enzyme. This result is also consistent with the previous research findings. Hartgerink et al. reported that specific enzyme cleavage sequence (MMP-2) containing peptide nanofiber gels were completely degraded at the end of one-month of incubation with collagenase IV in HEPES buffer. [82] On the other hand, the remaining weights were about 4% for the DL-E_3/K_3PA gels and no significant losses were observed for the D-E_3/K_3PA gels in the proteinase K containing solution. Control groups which were incubated with Tris buffer exhibited no noteworthy weight losses during the measurements. Interestingly, the results indicated that mixing the L- and the D-form peptide amphiphile molecules enhanced the stability of the gels against the enzymatic degradation.

To investigate the degradation of PA nanofibers specifically, dilute D-E_3/K_3, DL-E_3/K_3 and L-E_3/K_3 gel solutions (0.1 wt%, 100 μL) were incubated in 1 mg/mL Proteinase K (900 μL) solution and Tris buffer solution (900 μL). Proteinase K was selected as a model proteolytic enzyme to check the degradation of the peptide nanofibers. The samples were visualized by TEM at different time intervals to monitor any structural alteration and length difference that may happen during the proteolytic degradation. After 15 min incubation, the PNFs showed cylindrical fibers and no structural change except for the L-E_3/K_3in

enzyme containing media. There were both nanofiber and nanobelt like structures in the L-E_3/K_3 in proteinase K while the other groups demonstrated only long nanofiber networks. After 24 h of incubation, the lengths of the L-E_3/K_3 nanofibers decreased and they became broader in size. Possibly, the reason is that the degraded smaller peptide fragments are prone to come together or the salt effect of the buffer environment may influence the structure. At day 7, there were still significant declines in the lengths of the L-E_3/K_3nanofibers and increase in the diameters. Finally, only the small fragments of the PNFs were observed after 14 days of incubation with proteinase K. In addition, there were some widenings in sizes of nanofibers within Tris buffer at the day 14. The electrostatic interactions between amino acids and the buffer ions may promote aggregation of the L-form nanofibers during incubation time. (Figure 2.14)

The DL-E_3/K_3 nanofibers showed great stabilities against the enzymatic degradation in a similar fashion like the D- E_3/K_3. While the L-E_3/K_3 nanofibers were completely degraded after 14 days, they still preserved their overall structure. However, there were slight widenings in the sizes of the fibers over time. (Figure 2.15)

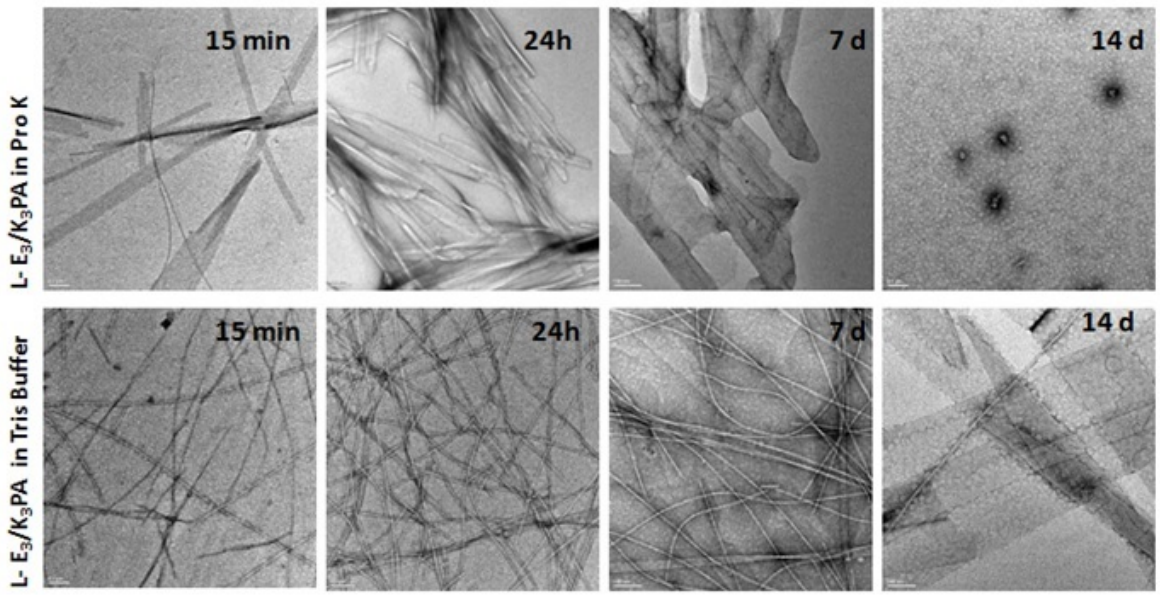

Figure 2.14: Degradation of L-E_3/K_3 peptide nanofibers visualized by TEM. TEM images of L-E_3/K_3 nanofibers incubated with 1 mg/mL proteinase K (top). TEM images of KRK peptide nanofibers incubated with Tris buffer (control). All scale bars are 100 nm.

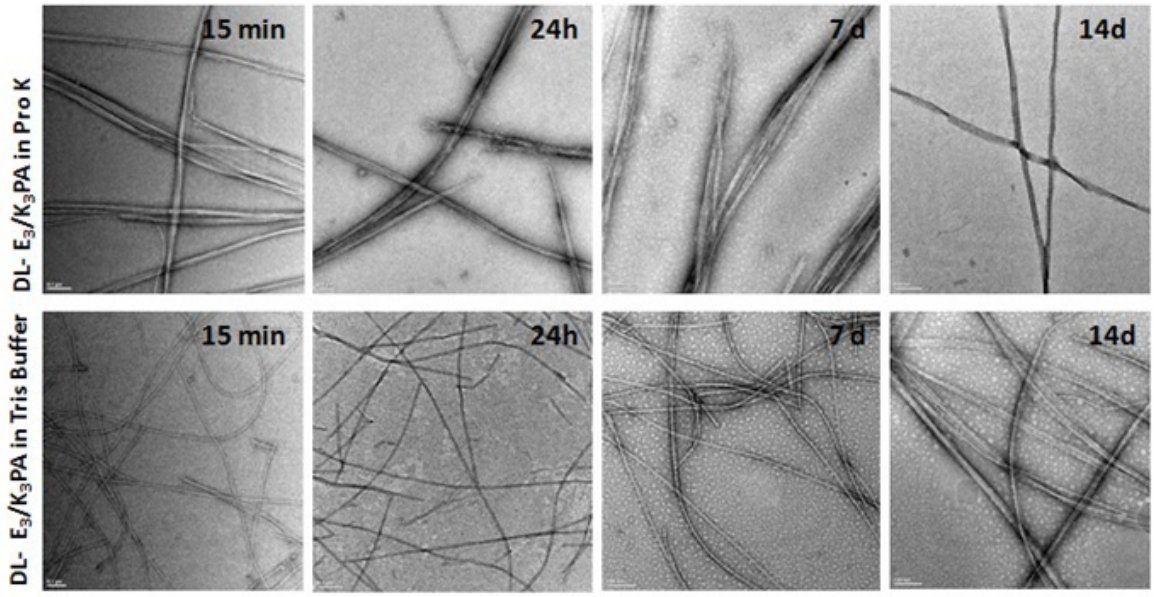

Figure 2.15: Degradation of DL-E_3/K_3 peptide nanofibers visualized by TEM. TEM images of DL-E_3/K_3 nanofibres incubated with 1 mg/mL proteinase K (top). TEM images of KRK peptide nanofibers incubated with Tris buffer (bottom). All scale bars are 100 nm

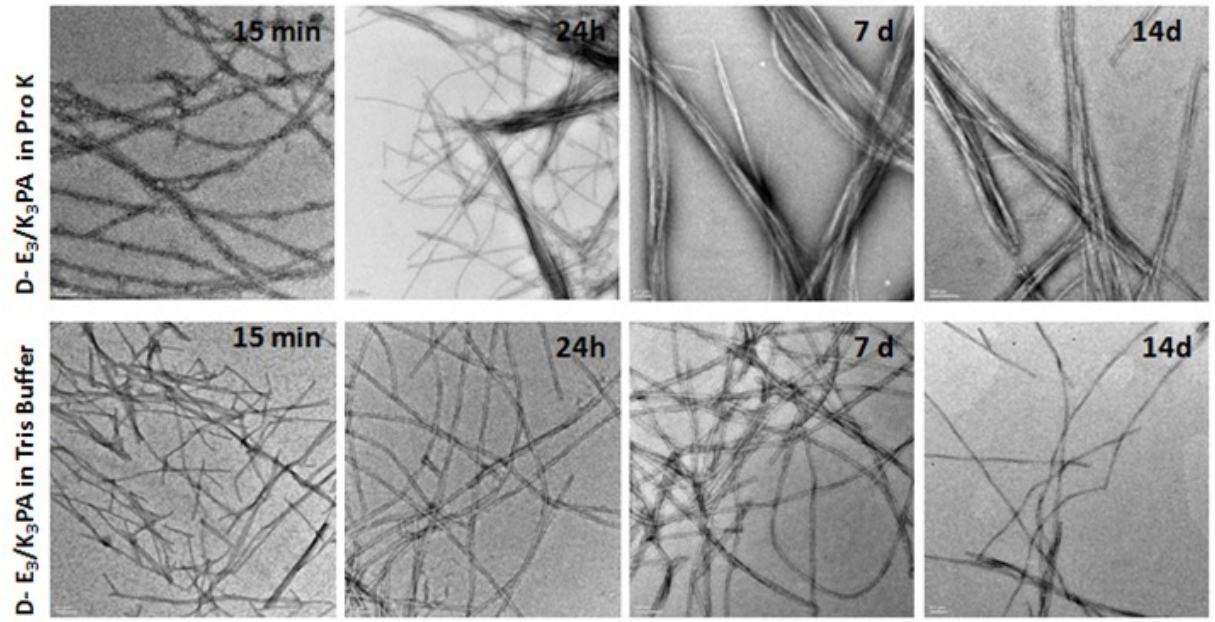

Figure 2.16: Degradation of D-E_3/K_3 peptide nanofibers visualized by TEM. TEM images of D-E_3/K_3 nanofibers incubated with 1 mg/mL proteinase K (top). TEM images of KRK peptide nanofibers incubated with Tris buffer (bottom). All scale bars are 100 nm.

As expected, the D-E_3/K_3 nanofibers were stable against the enzyme and had slight widenings in the sizes of the fibers during the incubation time. The control groups of the D-E_3/K_3 and the DL-E3/K3 nanofibers exhibited no significant change in length and structure of the nanofibers. (Figure 2.16)

In release studies, Rhodamine B dye was used as a tracer to understand the release behavior of three different gel matrices in enzyme and no enzyme containing environment. (Figure 2.17) The highest Rhodamine B release percentage was observed in the L-E_3/K_3 gels due to their tendencies towards the proteolytic degradation by proteinase K during 96h of incubation at room temperature. For the L-E_3/K_3 gels, % release in the enzyme containing environment was around 75%; for the D-E_3/K_3 gels, it was around 25% and for the DL-E_3/K_3 it was around 41%. In the Tris buffer containing environment, it can be seen that there was dramatic decrease in % release for the L-E_3/K_3 (34%) and the DL-E_3/K_3 (23%) gels compared with the D-E_3/K_3 gels (19%).

According to the results, proteinase K accelerated the degradation of self-assembled peptide gels by cleaving peptide bonds and this erosion increased release rate of Rhodamine B for 96 h. Since the D-form peptides are much more resistant to enzymatic degradation, the minimum release behavior was observed in the D-E_3/K_3PA gels as expected. The DL-E_3/K_3 gels showed two times higher release compared with the release of the D-E_3/K_3. In the presence of the enzyme, the L- form peptide amphiphile molecules inside the mixture may influence degradation and enhance release rate from the DL-E_3/K_3 gels.

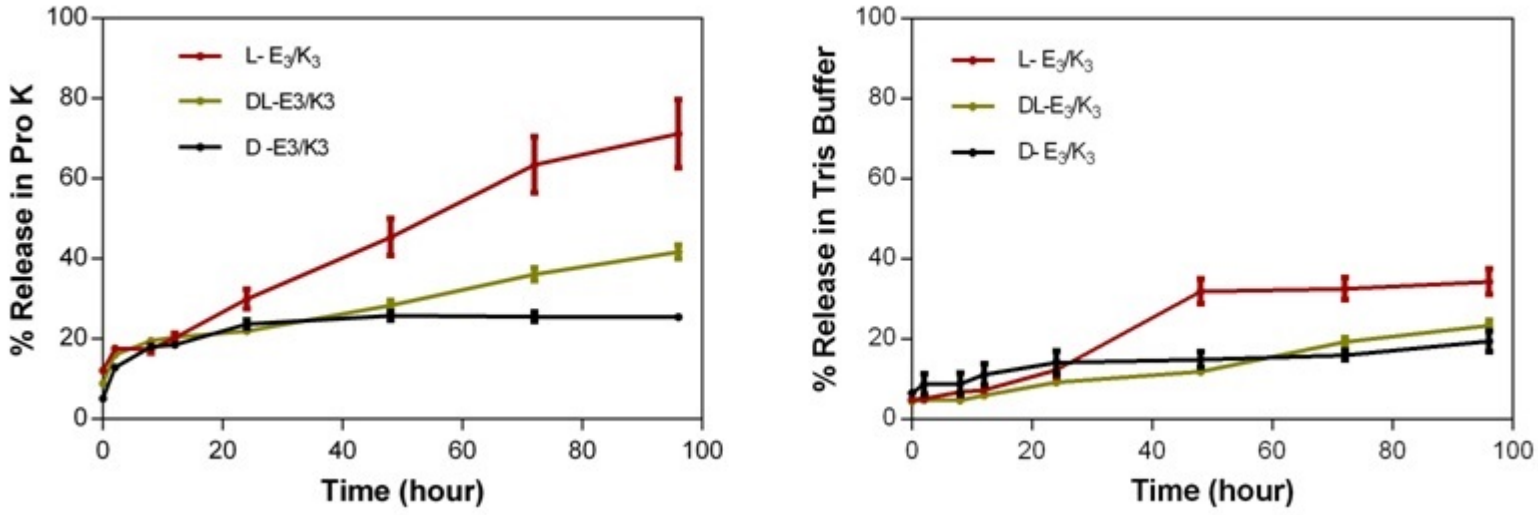

Figure 2.17: Rhodamine B release from self-assembled peptide gels (L-E3/K3, D-E3/K3 and DL-E3/K3) during 96 h

Chapter 3

Conclusions and Future Perspectives

3.1 Conclusions and Future Perspectives

Self-assembled peptide gels have captured great interest thanks to their inherent biocompatible, biodegradable and bioactive properties. They serve as an intelligent platform for various biomedical applications such as drug delivery, tissue engineering, wound healing.

Here, the self-assembled peptide amphiphile gels were formed by altering the ratio of L- to D-form peptide amphiphile molecules at physiological conditions. These 3D networks possess inherent biocompatibility and enable encapsulation of desired molecules such as drugs, or growth factors homogenously.

Various characterization techniques including LC-MS, CD, SEM, TEM and rheology were used to analyze the synthesized peptide amphiphile molecules. According to the LC-MS results, all of the peptide amphiphile molecules showed purities higher than 95% with molecular weights of 910 g/mol for the K_3PA and 912 g/mol for the E_3PA.

The CD results exhibited all of the samples were red-shifted relative to typical β-sheets with a maximum at 195 nm and a minimum at 216 nmat physiological pH. Mixture of these D- and L- form molecules (1:1 volume ratio) decreased the intensity of CD signal. Batch to batch variations in synthesis and excess TFA molecules which could not be removed from lysine residues may influence the intensity of this peak.

TEM imaging revealed co-assembly of these oppositely charged peptide amphiphiles and the mixtures of their chiral counterparts self-assemble into cylindrical nanofiber structures with diameters of about 6-10 nm. In addition, SEM imaging confirmed that 3D nanofiber networks of these gels are quite similar.

Oscillatory rheology was used to investigate the gelation kinetics and the viscoelastic properties of the PA gels. Time sweep test was performed to reveal the gelation kinetics within the linear viscoelastic region. Within 30 minutes, the storage moduli (G) of gels reached stationary phases which verify the complete

degradation. However, there were differences between the gels in terms of the required time to reach the plateaus. It took much longer for the DL-E_3/K_3 gels to reach the stationary phase compared to the time taken for the others. On the other hand, the/ D-E_3/K_3 and the L-E_3/K_3 gels reached to their plateaus approximately at the same time. The results also demonstrated that the storage moduli (G) of all the gel samples were significantly higher than their loss moduli (G), suggesting a solid-like rheological behavior and proving the gel formation during the self-assembly process. The D-E_3/K_3 and DL-E_3/K_3 gels have slightly higher storage moduli compared to the L-E_3/K_3. In order to investigate the viscoelastic properties of the PA gels, amplitude sweep test was employed. The results indicated that the increased strain values did not change the storage moduli of gels within the linear viscoelastic region. After exceeding the limiting strain amplitude (LSA), the storage moduli of the gels started to decrease while the employed strains were still increasing. This represents the transition from the linear to the nonlinear viscoelastic behavior. The weight loss based degradation method was used to investigate the proteolytic degradation profiles of the D-E_3/K_3PA, the DL-E_3/K_3PA and, the L-E_3/K_3PA gels in presence of proteinase K which is an effective protease catalyzing the hydrolysis of peptide bonds. The results clearly demonstrated that these gel matrices have altered susceptibilities to the enzymatic degradation. At the end of the incubation with proteinase K solution, the L-E_3/K_3PA gels lost approximately 80% of their weight, while this percentage was 4% for the DL-E_3/K_3PA gels. No weight loss was observed in the D-E_3/K_3PA gels in enzyme containing environment and the control groups. These results are interesting since the mixing L- and D- form peptide amphiphiles molecules enhanced the stability of gels against the enzymatic degradation significantly.

The degradations of the peptide nanofibers were visualized specifically by TEM at different time intervals. According to these result, the L-E_3/K_3PA was completely degraded after 14 days of incubation with proteinase K. Until the complete degradation, the lengths of the PA nanofibers were gradually decreased and there was a continuous broadening in the overall structure. The control groups of these nanofibers preserved their overall network structure until day 14. However, there were widenings in the size distributions of these nanofibers at the end of the day

14. The D-E_3/K_3PA and the DL-E_3/K_3PA nanofibers exhibited great stability in both enzyme and no enzyme containing environments. However, there was a slight widening in the sizes of the nanofibers.

In order to understand the influence of the PA gel degradation on release properties, UV-Vis microscopy was used to measure absorbance of Rhodamine B dye which is encapsulated within the PA gels network in enzyme and no enzyme containing environment. In presence of proteinase K, the highest Rhodamine B release percentage was observed in the L-E_3/K_3PA gels (75%). This value was around 25% for the D- E_3/K_3PA gels and 41% for the DL-E_3/K_3PA. There was significant reduction in % release for no enzyme containing environment particularly in the L-E_3/K_3PA (34%) and the DL-E_3/K_3PA (23%) gels. The D-E_3/K_3PA gels (19%) exhibited nearly the same release behavior. These findings are attractive for possible in vivo applications of these materials thanks to their tunable degradation profile and rigidity.

Bibliography

[1] A. Dasgupta, J. H. Mondal, and D. Das, "Peptide hydrogels," *Rsc Advances*, vol. 3, no. 24, pp. 9117–9149, 2013.

[2] L. Zhang, X. Wang, T. Wang, and M. Liu, "Tuning soft nanostructures in self-assembled supramolecular gels: From morphology control to morphology-dependent functions," *Small*, vol. 11, no. 9-10, pp. 1025–1038, 2015.

[3] Sigma-Aldrich, "Solid phase peptide synthesis description," 2015.

[4] S. M. Kelly, T. J. Jess, and N. C. Price, "How to study proteins by circular dichroism," *Biochimica et Biophysica Acta (BBA)-Proteins and Proteomics*, vol. 1751, no. 2, pp. 119–139, 2005.

[5] S. Kim, J. H. Kim, J. S. Lee, and C. B. Park, "Beta-sheet-forming, self-assembled peptide nanomaterials towards optical, energy, and healthcare applications," *Small*, vol. 11, no. 30, pp. 3623–3640, 2015.

[6] J. B. Matson and S. I. Stupp, "Self-assembling peptide scaffolds for regenerative medicine," *Chemical Communications*, vol. 48, no. 1, pp. 26–33, 2012.

[7] Y. S. Velichko, S. I. Stupp, and M. O. de la Cruz, "Molecular simulation study of peptide amphiphile self-assembly," *The journal of physical chemistry B*, vol. 112, no. 8, pp. 2326–2334, 2008.

[8] Z. Luo, X. Zhao, and S. Zhang, "Structural dynamic of a self-assembling peptide d-eak16 made of only d-amino acids," *PLoS One*, vol. 3, no. 5, p. e2364, 2008.

[9] J. Liu, L. Zhang, Z. Yang, and X. Zhao, "Controlled release of paclitaxel from a self-assembling peptide hydrogel formed in situ and antitumor study in vitro," 2011.

[10] J. Liu, J. Liu, L. Chu, Y. Zhang, H. Xu, D. Kong, Z. Yang, C. Yang, and D. Ding, "Self-assembling peptide of d-amino acids boosts selectivity and antitumor efficacy of 10-hydroxycamptothecin," *ACS applied materials & interfaces*, vol. 6, no. 8, pp. 5558–5565, 2014.

[11] M. Mazza, A. Patel, R. Pons, C. Bussy, and K. Kostarelos, "Peptide nanofibres as molecular transporters: from self-assembly to in vivo degradation," *Faraday discussions*, vol. 166, pp. 181–194, 2013.

[12] M. Rad-Malekshahi, L. Lempsink, M. Amidi, W. E. Hennink, and E. Mastrobattista, "Biomedical applications of self-assembling peptides," *Bioconjugate chemistry*, 2015.

[13] S. Zhang, "Fabrication of novel biomaterials through molecular self-assembly," *Nature biotechnology*, vol. 21, no. 10, pp. 1171–1178, 2003.

[14] X. Zhao, F. Pan, H. Xu, M. Yaseen, H. Shan, C. A. E. Hauser, S. Zhang, and J. R. Lu, "Molecular self-assembly and applications of designer peptide amphiphiles," *Chem. Soc. Rev.*, vol. 39, pp. 3480–3498, 2010.

[15] D. Mandal, A. N. Shirazi, and K. Parang, "Self-assembly of peptides to nanostructures," *Organic & biomolecular chemistry*, vol. 12, no. 22, pp. 3544–3561, 2014.

[16] S. Toksöz and M. O. Guler, "Self-assembled peptidic nanostructures," *Nano Today*, vol. 4, no. 6, pp. 458–469, 2009.

[17] R. B. Merrifield, "Solid phase peptide synthesis. i. the synthesis of a tetrapeptide," *Journal of the American Chemical Society*, vol. 85, no. 14, pp. 2149–2154, 1963.

[18] R. Merrifield, "Solid-phase peptide synthesis," *Advances in Enzymology and Related Areas of Molecular Biology, Volume 32*, pp. 221–296, 2006.

[19] S.-S. Wang, "p-alkoxybenzyl alcohol resin and p-alkoxybenzyloxycarbonylhydrazide resin for solid phase synthesis of protected peptide fragments," *Journal of the American Chemical Society*, vol. 95, no. 4, pp. 1328–1333, 1973.

[20] S.-S. Wang, "p-alkoxybenzyl alcohol resin and p-alkoxybenzyloxycarbonylhydrazide resin for solid phase synthesis of protected peptide fragments," *Journal of the American Chemical Society*, vol. 95, no. 4, pp. 1328–1333, 1973.

[21] K. Barlos and D. Gatos, "9-fluorenylmethyloxycarbonyl/tbutyl-based convergent protein synthesis," *Peptide Science*, vol. 51, no. 4, pp. 266–278, 1999.

[22] G. B. Fields and R. L. NOBLE, "Solid phase peptide synthesis utilizing 9-fluorenylmethoxycarbonyl amino acids," *International journal of peptide and protein research*, vol. 35, no. 3, pp. 161–214, 1990.

[23] J. P. Pellois, W. Wang, and X. Gao, "Peptide synthesis based on t-boc chemistry and solution photogenerated acids," *Journal of combinatorial chemistry*, vol. 2, no. 4, pp. 355–360, 2000.

[24] M. SCHNölzer, P. ALEWOOD, A. JONES, D. ALEWOOD, and S. B. KENT, "In situ neutralization in boc-chemistry solid phase peptide synthesis," *International journal of peptide and protein research*, vol. 40, no. 3-4, pp. 180–193, 1992.

[25] E. Atherton, H. Fox, D. Harkiss, C. Logan, R. Sheppard, and B. Williams, "A mild procedure for solid phase peptide synthesis: use of fluorenylmethoxycarbonylamino-acids," *Journal of the Chemical Society, Chemical Communications*, no. 13, pp. 537–539, 1978.

[26] M. DHondt, N. Bracke, L. Taevernier, B. Gevaert, F. Verbeke, E. Wynendaele, and B. De Spiegeleer, "Related impurities in peptide medicines," *Journal of pharmaceutical and biomedical analysis*, vol. 101, pp. 2–30, 2014.

[27] M. Liu, L. Zhang, and T. Wang, "Supramolecular chirality in self-assembled systems," *Chemical Reviews*, vol. 115, no. 15, pp. 7304–7397, 2015.

[28] E. Gazit, "Self-assembled peptide nanostructures: the design of molecular building blocks and their technological utilization," *Chemical Society Reviews*, vol. 36, no. 8, pp. 1263–1269, 2007.

[29] S. Bulut, T. S. Erkal, S. Toksoz, A. B. Tekinay, T. Tekinay, and M. O. Guler, "Slow release and delivery of antisense oligonucleotide drug by self-assembled peptide amphiphile nanofibers," *Biomacromolecules*, vol. 12, no. 8, pp. 3007–3014, 2011.

[30] P. Zhang, A. G. Cheetham, Y.-a. Lin, and H. Cui, "Self-assembled tat nanofibers as effective drug carrier and transporter," *ACS nano*, vol. 7, no. 7, pp. 5965–5977, 2013.

[31] M. R. Ghadiri and J. R. Granja, "Artificial transmembrane ion channels from self-assembling," *Nature*, vol. 369, p. 26, 1994.

[32] M. Reches and E. Gazit, "Casting metal nanowires within discrete self-assembled peptide nanotubes," *Science*, vol. 300, no. 5619, pp. 625–627, 2003.

[33] M. Yemini, M. Reches, J. Rishpon, and E. Gazit, "Novel electrochemical biosensing platform using self-assembled peptide nanotubes," *Nano Letters*, vol. 5, no. 1, pp. 183–186, 2005.

[34] S. R. Bull, M. O. Guler, R. E. Bras, T. J. Meade, and S. I. Stupp, "Self-assembled peptide amphiphile nanofibers conjugated to mri contrast agents," *Nano Letters*, vol. 5, no. 1, pp. 1–4, 2005.

[35] E. Arslan, I. C. Garip, G. Gulseren, A. B. Tekinay, and M. O. Guler, "Bioactive supramolecular peptide nanofibers for regenerative medicine," *Advanced healthcare materials*, vol. 3, no. 9, pp. 1357–1376, 2014.

[36] X. Zhao and S. Zhang, "Molecular designer self-assembling peptides," *Chemical Society Reviews*, vol. 35, no. 11, pp. 1105–1110, 2006.

[37] H. Cui, M. J. Webber, and S. I. Stupp, "Self-assembly of peptide amphiphiles: From molecules to nanostructures to biomaterials," *Peptide Science*, vol. 94, no. 1, pp. 1–18, 2010.

[38] S. Toksöz and M. O. Guler, "Self-assembled peptidic nanostructures," *Nano Today*, vol. 4, no. 6, pp. 458–469, 2009.

[39] S. E. Paramonov, H.-W. Jun, and J. D. Hartgerink, "Self-assembly of peptide-amphiphile nanofibers: the roles of hydrogen bonding and amphiphilic packing," *Journal of the American Chemical Society*, vol. 128, no. 22, pp. 7291–7298, 2006.

[40] X. Zhang and C. Wang, "Supramolecular amphiphiles," *Chemical Society Reviews*, vol. 40, no. 1, pp. 94–101, 2011.

[41] G. A. Silva, C. Czeisler, K. L. Niece, E. Beniash, D. A. Harrington, J. A. Kessler, and S. I. Stupp, "Selective differentiation of neural progenitor cells by high-epitope density nanofibers," *Science*, vol. 303, no. 5662, pp. 1352–1355, 2004.

[42] K. L. Niece, J. D. Hartgerink, J. J. Donners, and S. I. Stupp, "Self-assembly combining two bioactive peptide-amphiphile molecules into nanofibers by electrostatic attraction," *Journal of the American Chemical Society*, vol. 125, no. 24, pp. 7146–7147, 2003.

[43] H. Hosseinkhani, P.-D. Hong, and D.-S. Yu, "Self-assembled proteins and peptides for regenerative medicine," *Chemical reviews*, vol. 113, no. 7, pp. 4837–4861, 2013.

[44] J. C. Stendahl, M. S. Rao, M. O. Guler, and S. I. Stupp, "Intermolecular forces in the self-assembly of peptide amphiphile nanofibers," *Advanced Functional Materials*, vol. 16, no. 4, pp. 499–508, 2006.

[45] I. Hamley, "Self-assembly of amphiphilic peptides," *Soft Matter*, vol. 7, no. 9, pp. 4122–4138, 2011.

[46] S. Toksoz, R. Mammadov, A. B. Tekinay, and M. O. Guler, "Electrostatic effects on nanofiber formation of self-assembling peptide amphiphiles," *Journal of colloid and interface science*, vol. 356, no. 1, pp. 131–137, 2011.

[47] S. Han, S. Cao, Y. Wang, J. Wang, D. Xia, H. Xu, X. Zhao, and J. R. Lu, "Self-assembly of short peptide amphiphiles: The cooperative effect of hydrophobic interaction and hydrogen bonding," *Chemistry–A European Journal*, vol. 17, no. 46, pp. 13095–13102, 2011.

[48] J. D. Hartgerink, E. Beniash, and S. I. Stupp, "Peptide-amphiphile nanofibers: a versatile scaffold for the preparation of self-assembling materials," *Proceedings of the National Academy of Sciences*, vol. 99, no. 8, pp. 5133–5138, 2002.

[49] H. Cui, M. J. Webber, and S. I. Stupp, "Self-assembly of peptide amphiphiles: From molecules to nanostructures to biomaterials," *Peptide Science*, vol. 94, no. 1, pp. 1–18, 2010.

[50] S. Zhang, C. Lockshin, A. Herbert, E. Winter, and A. Rich, "Zuotin, a putative z-dna binding protein in saccharomyces cerevisiae.," *The EMBO journal*, vol. 11, no. 10, p. 3787, 1992.

[51] S. Marqusee and R. L. Baldwin, "Helix stabilization by glu-... lys+ salt bridges in short peptides of de novo design," *Proceedings of the National Academy of Sciences*, vol. 84, no. 24, pp. 8898–8902, 1987.

[52] S. Marqusee, V. H. Robbins, and R. L. Baldwin, "Unusually stable helix formation in short alanine-based peptides," *Proceedings of the National Academy of Sciences*, vol. 86, no. 14, pp. 5286–5290, 1989.

[53] S. Zhang, T. Holmes, C. Lockshin, and A. Rich, "Spontaneous assembly of a self-complementary oligopeptide to form a stable macroscopic membrane.," *Proceedings of the National Academy of Sciences*, vol. 90, no. 8, pp. 3334–3338, 1993.

[54] Z. Luo, S. Wang, and S. Zhang, "Fabrication of self-assembling d-form peptide nanofiber scaffold d-eak16 for rapid hemostasis," *Biomaterials*, vol. 32, no. 8, pp. 2013–2020, 2011.

[55] Z. Luo, Y. Yue, Y. Zhang, X. Yuan, J. Gong, L. Wang, B. He, Z. Liu, Y. Sun, J. Liu, *et al.*, "Designer d-form self-assembling peptide nanofiber scaffolds

for 3-dimensional cell cultures," *Biomaterials*, vol. 34, no. 21, pp. 4902–4913, 2013.

[56] G. Fichman and E. Gazit, "Self-assembly of short peptides to form hydrogels: Design of building blocks, physical properties and technological applications," *Acta biomaterialia*, vol. 10, no. 4, pp. 1671–1682, 2014.

[57] J. L. Drury and D. J. Mooney, "Hydrogels for tissue engineering: scaffold design variables and applications," *Biomaterials*, vol. 24, no. 24, pp. 4337–4351, 2003.

[58] Y. Li, J. Rodrigues, and H. Tomás, "Injectable and biodegradable hydrogels: gelation, biodegradation and biomedical applications," *Chemical Society Reviews*, vol. 41, no. 6, pp. 2193–2221, 2012.

[59] S. Toledano, R. J. Williams, V. Jayawarna, and R. V. Ulijn, "Enzyme-triggered self-assembly of peptide hydrogels via reversed hydrolysis," *Journal of the American Chemical Society*, vol. 128, no. 4, pp. 1070–1071, 2006.

[60] J. H. Collier, B.-H. Hu, J. W. Ruberti, J. Zhang, P. Shum, D. H. Thompson, and P. B. Messersmith, "Thermally and photochemically triggered self-assembly of peptide hydrogels," *Journal of the American Chemical Society*, vol. 123, no. 38, pp. 9463–9464, 2001.

[61] E. Gazit, "Self-assembled peptide nanostructures: the design of molecular building blocks and their technological utilization," *Chemical Society Reviews*, vol. 36, no. 8, pp. 1263–1269, 2007.

[62] A. M. Jonker, D. W. Lowik, and J. C. van Hest, "Peptide-and protein-based hydrogels," *Chemistry of Materials*, vol. 24, no. 5, pp. 759–773, 2012.

[63] J.-A. Yang, J. Yeom, B. W. Hwang, A. S. Hoffman, and S. K. Hahn, "In situ-forming injectable hydrogels for regenerative medicine," *Progress in Polymer Science*, vol. 39, no. 12, pp. 1973–1986, 2014.

[64] R. Orbach, L. Adler-Abramovich, S. Zigerson, I. Mironi-Harpaz, D. Seliktar, and E. Gazit, "Self-assembled fmoc-peptides as a platform for the formation of nanostructures and hydrogels," *Biomacromolecules*, vol. 10, no. 9, pp. 2646–2651, 2009.

[65] W. Wang, "Instability, stabilization, and formulation of liquid protein pharmaceuticals," *International journal of pharmaceutics*, vol. 185, no. 2, pp. 129–188, 1999.

[66] N. Jenkins, "Modifications of therapeutic proteins: challenges and prospects," *Cytotechnology*, vol. 53, no. 1-3, pp. 121–125, 2007.

[67] T. W. Randolph and J. F. Carpenter, "Engineering challenges of protein formulations," *AIChE journal*, vol. 53, no. 8, pp. 1902–1907, 2007.

[68] Y. Shi and L. Li, "Current advances in sustained-release systems for parenteral drug delivery," *Expert opinion on drug delivery*, vol. 2, no. 6, pp. 1039–1058, 2005.

[69] N. A. Peppas, J. Z. Hilt, A. Khademhosseini, and R. Langer, "Hydrogels in biology and medicine: from molecular principles to bionanotechnology," *Advanced Materials*, vol. 18, no. 11, pp. 1345–1360, 2006.

[70] M. J. Webber, E. J. Berns, and S. I. Stupp, "Supramolecular nanofibers of peptide amphiphiles for medicine," *Israel journal of chemistry*, vol. 53, no. 8, pp. 530–554, 2013.

[71] S. Majumdar and T. J. Siahaan, "Peptide-mediated targeted drug delivery," *Medicinal research reviews*, vol. 32, no. 3, pp. 637–658, 2012.

[72] R. Soudy, C. Chen, and K. Kaur, "Novel peptide–doxorubucin conjugates for targeting breast cancer cells including the multidrug resistant cells," *Journal of medicinal chemistry*, vol. 56, no. 19, pp. 7564–7573, 2013.

[73] J.-K. Kim, J. Anderson, H.-W. Jun, M. A. Repka, and S. Jo, "Self-assembling peptide amphiphile-based nanofiber gel for bioresponsive cisplatin delivery," *Molecular pharmaceutics*, vol. 6, no. 3, pp. 978–985, 2009.

[74] J.-K. Kim, J. Anderson, H.-W. Jun, M. A. Repka, and S. Jo, "Self-assembling peptide amphiphile-based nanofiber gel for bioresponsive cisplatin delivery," *Molecular pharmaceutics*, vol. 6, no. 3, pp. 978–985, 2009.

[75] B. Amsden, "Solute diffusion within hydrogels. mechanisms and models," *Macromolecules*, vol. 31, no. 23, pp. 8382–8395, 1998.

[76] J. Siepmann and N. Peppas, "Modeling of drug release from delivery systems based on hydroxypropyl methylcellulose (hpmc)," *Advanced drug delivery reviews*, vol. 64, pp. 163–174, 2012.

[77] C.-C. Lin and A. T. Metters, "Hydrogels in controlled release formulations: network design and mathematical modeling," *Advanced drug delivery reviews*, vol. 58, no. 12, pp. 1379–1408, 2006.

[78] R. Bettini, P. Colombo, G. Massimo, P. L. Catellani, and T. Vitali, "Swelling and drug release in hydrogel matrices: polymer viscosity and matrix porosity effects," *European Journal of Pharmaceutical Sciences*, vol. 2, no. 3, pp. 213–219, 1994.

[79] N. A. Peppas, J. Z. Hilt, A. Khademhosseini, and R. Langer, "Hydrogels in biology and medicine: from molecular principles to bionanotechnology," *Advanced Materials*, vol. 18, no. 11, pp. 1345–1360, 2006.

[80] N. Peppas, P. Bures, W. Leobandung, and H. Ichikawa, "Hydrogels in pharmaceutical formulations," *European journal of pharmaceutics and biopharmaceutics*, vol. 50, no. 1, pp. 27–46, 2000.

[81] Y. Zhao, M. Tanaka, T. Kinoshita, M. Higuchi, and T. Tan, "Self-assembling peptide nanofiber scaffolds for controlled release governed by gelator design and guest size," *Journal of Controlled Release*, vol. 147, no. 3, pp. 392–399, 2010.

[82] H.-W. Jun, V. Yuwono, S. E. Paramonov, and J. D. Hartgerink, "Enzyme-mediated degradation of peptide-amphiphile nanofiber networks," *Advanced Materials*, vol. 17, no. 21, pp. 2612–2617, 2005.

[83] A. Barnard and D. K. Smith, "Self-assembled multivalency: Dynamic ligand arrays for high-affinity binding," *Angewandte Chemie International Edition*, vol. 51, no. 27, pp. 6572–6581, 2012.

[84] J. Boekhoven, A. M. Brizard, K. N. Kowlgi, G. J. Koper, R. Eelkema, and J. H. van Esch, "Dissipative self-assembly of a molecular gelator by using a chemical fuel," *Angewandte Chemie International Edition*, vol. 49, no. 28, pp. 4825–4828, 2010.

[85] X. Miao, W. Cao, W. Zheng, J. Wang, X. Zhang, J. Gao, C. Yang, D. Kong, H. Xu, L. Wang, *et al.*, "Switchable catalytic activity: Selenium-containing peptides with redox-controllable self-assembly properties," *Angewandte Chemie International Edition*, vol. 52, no. 30, pp. 7781–7785, 2013.

[86] G. Liang, Z. Yang, R. Zhang, L. Li, Y. Fan, Y. Kuang, Y. Gao, T. Wang, W. W. Lu, and B. Xu, "Supramolecular hydrogel of a d-amino acid dipeptide for controlled drug release in vivo," *Langmuir*, vol. 25, no. 15, pp. 8419–8422, 2009.

[87] X. Li, X. Du, J. Li, Y. Gao, Y. Pan, J. Shi, N. Zhou, and B. Xu, "Introducing d-amino acid or simple glycoside into small peptides to enable supramolecular hydrogelators to resist proteolysis," *Langmuir*, vol. 28, no. 37, pp. 13512–13517, 2012.

[88] C. Yang, L. Chu, Y. Zhang, Y. Shi, J. Liu, Q. Liu, S. Fan, Z. Yang, D. Ding, D. Kong, *et al.*, "Dynamic biostability, biodistribution, and toxicity of l/d-peptide-based supramolecular nanofibers," *ACS applied materials & interfaces*, vol. 7, no. 4, pp. 2735–2744, 2015.